


Please cite the Published Version

Zhang, Cheng, Wang, Juan, Song, Xiaoye, Yu, Deen, Guo, Baoqiang , Pang, Yaoyu, Yin, Xiaomei, Zhao, Shasha, Deng, Huan, Zhang, Shihua and Deng, Wensheng (2023) STAT3 potentiates RNA polymerase I-directed transcription and tumor growth by activating RPA34 expression. *British Journal of Cancer*, 128 (5). pp. 766-782. ISSN 0007-0920

DOI: <https://doi.org/10.1038/s41416-022-02098-6>

Publisher: Springer Nature [academic journals on nature.com]

Version: Accepted Version

Downloaded from: <https://e-space.mmu.ac.uk/632936/>

Usage rights:  In Copyright

Additional Information: This version of the article has been accepted for publication, after peer review (when applicable) and is subject to Springer Nature's AM terms of use (<https://www.springernature.com/gp/open-research/policies/accepted-manuscript-terms>), but is not the Version of Record and does not reflect post-acceptance improvements, or any corrections. The Version of Record is available online at: <http://dx.doi.org/10.1038/s41416-022-02098-6>

Enquiries:

If you have questions about this document, contact openresearch@mmu.ac.uk. Please include the URL of the record in e-space. If you believe that your, or a third party's rights have been compromised through this document please see our Take Down policy (available from <https://www.mmu.ac.uk/library/using-the-library/policies-and-guidelines>)

1 **STAT3 potentiates RNA polymerase I-directed transcription** 2 **and tumor growth by activating RPA34 expression**

3 Cheng Zhang¹, Juan Wang^{1,2}, Xiaoye Song¹, Deen Yu¹, Baoqiang Guo³, Yaoyu Pang⁴,
4 Xiaomei Yin¹, Shasha Zhao^{1,*}, Huan Deng^{1,*}, Shihua Zhang^{1,*}, Wensheng Deng^{1,*}

5 ¹School of Life Science and Health, Wuhan University of Science and Technology,
6 Wuhan, 430065

7 ²School of Materials and Metallurgy, Wuhan University of Science and Technology,
8 Wuhan, 430081

9 ³Department of Life Sciences, Manchester Metropolitan University, Manchester, M15
10 6BH, UK

11 ⁴Institute of Systems, Molecular and Integrative Biology, University of Liverpool,
12 Liverpool, L69 7GE, UK

13
14 * Correspondence:

15 zhaoshasha@wust.edu.cn; denghuan@wust.edu.cn; zhangshihua@wust.edu.cn;
16 dengwensheng@wust.edu.cn

17
18 **Short title:** STAT3 & Pol I-directed transcription

23 **Abstract**

24 **Background:** Deregulation of either RNA polymerase I (Pol I)-directed transcription
25 or expression of signal transducer and activator of transcription 3 (STAT3) correlates
26 closely with tumorigenesis. However, the connection between STAT3 and Pol I-
27 directed transcription hasn't been investigated.

28 **Methods:** The role of STAT3 in Pol I-directed transcription was determined using
29 combined techniques. The regulation of tumor cell growth mediated by STAT3 and
30 Pol I products was analyzed *in vitro* and *in vivo*. RNAseq, CHIP assays and rescue
31 assays were used to uncover the mechanism of Pol I transcription mediated by
32 STAT3.

33 **Results:** STAT3 expression positively correlates with Pol I product levels and cancer
34 cell growth. The inhibition of STAT3 or Pol I products suppresses cell growth.
35 Mechanistically, STAT3 activates Pol I-directed transcription by enhancing the
36 recruitment of the Pol I transcription machinery to the rDNA promoter. STAT3
37 directly activates *Rpa34* gene transcription by binding to the *RPA34* promoter, which
38 enhances the occupancies of the Pol II transcription machinery factors at this
39 promoter. Cancer patients with RPA34 high expression lead to poor survival
40 probability and short survival time.

41 **Conclusion:** STAT3 potentiates Pol I-dependent transcription and tumor cell growth

42 by activating RPA34 *in vitro* and *in vivo*.

43 **Keywords:** STAT3, RNA polymerase I, ribosomal rRNA expression, tumor growth,
44 RPA34

45 **Background**

46 Signal transducer and activator of transcription 3 (STAT3) is a member of the STAT
47 family that regulates numerous biological processes, including cell proliferation and
48 migration, apoptosis, angiogenesis, immunosuppression and cancer stem cell
49 maintenance [1-3]. STAT3 can be activated by several canonical signaling pathways
50 such as IL6/JAK, EGF/EGFR and ABL/SRC pathways [2, 4, 5]. After activation,
51 STAT3 is phosphorylated, dimerized and translocated to the nucleus through its
52 nuclear localization sequence, where it binds to STAT3 consensus sequences to
53 activate transcription of its target genes [2, 6, 7]. Numerous studies have shown that
54 STAT3 is also localized to mitochondria and regulates mitochondrial respiration by
55 interacting with components of the electron transport chain (ETC) [8-12]. In addition
56 to the roles in mitochondrial, another non-canonical role of STAT3 is that
57 unphosphorylated STAT3 (uSTAT3) can enter the nucleus and bind to the GAS
58 promoter sequence to modulate transcription [2, 13]. The uSTAT3 contributes to
59 cancer progression by increasing STAT3 transcription activity. Activation of *Stat3*
60 gene transcription by IL-6 signaling augments uSTAT3 production, which promotes
61 expression of *E2f1*, *Met* and *Mras* genes [15, 16]. Recently, many novel activators of
62 STAT3, including lncRNA, miRNA, circRNA and proteins, have been identified [3,
63 17-25]. Some of them have been confirmed to be promising targets for anti-cancer
64 therapy [3, 26-29]. Cai G et al reported that an inhibitor called SD-36 can act as a
65 potent and selective degrader of STAT3 to inhibit the growth of a subset of acute
66 myeloid leukemia by inducing cell cycle arrest [30]. Another inhibitor STAT3-IN-3
67 has been confirmed to repress tumor growth for breast cancer cell line 4T1
68 xenografted in mice by reducing proliferative activity [31]. It has been shown that
69 constitutively activated STAT3 can promote cell proliferation by increasing the
70 expression of CyclinD1, c-Myc and Survivin [32-34]. However, how STAT3
71 activation enhances cell proliferation is not fully understood.

72 Human RNA polymerase I (Pol I) is responsible for the synthesis of 45S pre-rRNA,
73 which is instantly processed into 28S, 18S and 5.8S rRNA. Pol I products are
74 essential to ribosomal assembly, protein synthesis and cell growth [35, 36].

75 Abnormally high levels of Pol I products have been observed in a subset of cancer
76 tissues [37]. Pol I-directed transcription is tightly controlled by many factors,
77 including Pol I general transcription factors, oncogenic factors, tumor suppressors,
78 signaling pathways, chromatin modification and non-coding RNAs [38-43]. Despite
79 massive advances in the research field of Pol I-directed transcription, the regulatory
80 pathways and factors controlling this process remain to be identified. In our previous
81 work, we showed that cytoskeletal filamin A (FLNA) silencing enhanced Pol I-
82 directed transcription and cell proliferation [44]. Recently, RNA-seq analysis revealed
83 that FLNA silencing reduced STAT3 mRNA expression in tumor cell lines. Whether
84 STAT3 is associated with Pol I-dependent transcription hasn't been investigated. In

85 this study, we showed that STAT3 functions as a positive factor in the regulation of
86 Pol I-directed transcription and tumor cell survival and growth. We investigated the
87 effect of an STAT3 inhibitor and Pol I-specific inhibitors on tumor cell growth *in vitro*
88 and *in vivo* and explored the regulatory mechanisms of Pol I transcription mediated by
89 STAT3.

90 **Materials & Methods**

91 *Plasmids, cells, and reagents*

92 Three distinct DNA fragments encoding STAT3 shRNA molecules were
93 synthesized by Sangon Biotech (Shanghai, China) and inserted downstream of the U6
94 promoter at the pLVU6-EGFP-Puro plasmid (Inovogen, Beijing, China). STAT3 and
95 RPA34 cDNA fragments were inserted immediately downstream of the mCherry gene
96 at the pLVEF1 α -mCherry-Puro plasmid (Inovogen, Beijing, China). The rDNA
97 promoter along with a piece of cDNA encoding a small fragment of 45S rRNA near
98 the 5' prime was loaded into the pGL3-basic reporter vector. Cell lines, including
99 SaOS2, HeLa, 293T and HepG2, were purchased from American Type Cell Collection
100 (ATCC, USA) and cultured their corresponding medium supplied with 10% FBS
101 (Thermo Scientific, USA) and 1 \times Penicillin/ Streptomycin (GE Healthcare). After
102 culturing 48 hours, mycoplasma contamination tests were performed and STR (short
103 tandem repeat) profiling was performed. Restriction enzymes were purchased from
104 New England Biolab (USA). Biological reagents such as transfection and Western
105 blot detection reagents were obtained from Thermo Scientific (USA). The chemicals
106 used in this study were purchased from Sigma-Aldrich (Merk).

107 *Transfection and cell line generation*

108 Three distinct double-strand siRNA fragments that interfere with STAT3 expression
109 were synthesized by Genewiz Co (Shuzhou, China). HeLa and HepG2 cells were
110 cultured for 24 hours in 12-well plates, transient transfection for cells in each well
111 was performed using the mixture of 2 μ L Turbofect (Thermo Scientific) and 60
112 pmoles siRNA (20 pmoles for each siRNA). Forty-eight hours post-transfection,
113 STAT3 and ribosomal RNA expression were analyzed by Western blot and RT-qPCR,
114 respectively. For the generation of cell lines with STAT3 knockdown or
115 overexpression, the medium containing lentiviral particles was initially prepared by
116 transfecting 293T cells with 40 μ g lentiviral vectors expressing STAT3 shRNA- or
117 mCherry-STAT3 and packaging vectors pH1 (30 μ g) and pH2 (10 μ g). The resulting
118 medium was used for the transduction of HeLa, HepG2 and 293T cells. Cells were
119 selected with puromycin, and stable cell lines with STAT3 silencing and
120 overexpression were verified by RT-qPCR and Western blot. For the generation of the
121 cell lines concurrently expressing STAT3 shRNA and mCherry-RPA34, lentiviral
122 particles expressing mCherry-STAT3 were used for the transduction of the STAT3-
123 depleted cell lines, and the rest of the protocol followed the procedures as described
124 above.

125 *Endogenous protein activation and repression assays mediated by CRISPR dCas9- 126 KRAB/VP48 and STAT3 inhibitor assays*

127 Two DNA fragments encoding the guide RNA molecules targeting different

128 positions at the *STAT3* promoter were synthesized by Sangon (Shanghai, China) and
129 inserted downstream of the U6 promoter at the pLVU6-sgRNA-hUbC-dCas9-KRAB
130 vector (Cat No. 71236, Addgene, USA) or the pAC2-dual-dCas9VP48-sgExpression
131 vector (Cat No. 48236, Addgene, USA). The resulting vectors were transiently
132 transfected into HepG2 cells; after 48 hours, cells were harvested, and STAT3 and
133 ribosomal RNA were detected by Western blot and RT-qPCR, respectively. For the
134 assays with a STAT3 inhibitor, two groups of HeLa or HepG2 cells were cultured for
135 24 hours before the STAT3 inhibitor was added into one group of cells at a final
136 concentration of 2 μ M, meanwhile, DMSO was added into another group of cells.
137 After 48 hours, STAT3 expression and phosphorylation were analyzed by Western
138 blot using an anti-STAT3 antibody (CST#9139, CST, USA) and an anti-p-STAT3
139 antibody (CSB-PA004932LA01HU, CUSABio, China), while ribosomal RNA
140 expression was detected by RT-qPCR. .

141 *Immunofluorescence assays*

142 HeLa or HepG2 cells were cultured on small round coverslips (14 mm in diameter)
143 in the complete medium. When growing up to 60% of culturing surface, cells were
144 fixed for 10 min with 4% formaldehyde freshly prepared with 1 \times PBS solution. After
145 fixation, immunofluorescence (IF) assays were performed as described previously
146 [45] using the antibodies against STAT3 and RPA34 (CSB-PA006734, CUSABio,
147 China) and nucleolar protein markers (Fibrillarin, Ab66630, Ab4566, Abcam, UK).
148 IF assays for HepG2 cell lines expressing STAT3 shRNA or control shRNA were
149 performed using antibodies against RPA34 and Fibrillarin. Cell specimens were
150 observed under a confocal fluorescence microscope, and images were captured with a
151 60 \times objective lens (Olympus). The resulting images were analyzed with ImageJ
152 software (NIH).

153 *RT-qPCR and 5-ethynyl uridine assays*

154 HeLa and HepG2 cell lines expressing STAT3 shRNA or mCherry-STAT3 and their
155 control cell lines were cultured in 6-well plates using their corresponding culture
156 medium. At 90% confluence, cells were harvested and total RNA was extracted from
157 the cells using the RNA extraction kit (Axygen). The expression of both *STAT3* and
158 ribosomal RNA genes was analyzed by RT-qPCR as described previously [44, 45].
159 For 5-ethynyl uridine (EU) assays, HeLa or HepG2 cells were cultured and labelled
160 with EU for 2 hours; after labeling, cells were fixed with a 4 % formaldehyde solution
161 and EU-labeled cells were detected using the Cell-Light EU Apollo 555 (or 488)
162 Imaging Kit (RiboBio, Guangzhou). Cell samples were observed under a confocal
163 fluorescence microscope (Olympus, Japan), and images were captured with a
164 20 \times objective lens. The fluorescence intensity for nucleoli or nucleoplasm area was
165 obtained with the Image J software. The relative fluorescence intensity for a nucleolus
166 was obtained using the following formula: (the fluorescence intensity of a nucleolus –
167 the fluorescence intensity of the equal area of nucleoplasm) \times the rate of Pol I
168 products in total rRNA (0.983). The data from EU assays were analyzed by the
169 ImageJ and Graphpad Prism 8 software.

170 *Dot blotting*

171 HepG2 cell lines expressing STAT3 shRNA or mCherry-STAT3 and the

172 corresponding control cell lines were cultured in 10 cm dishes. At 90% confluence,
173 cells were harvested and nuclei were purified from the cells. Next, total RNA was
174 extracted from nuclei using an RNA extraction kit (Axygen). One microgram of total
175 RNA was loaded in individual circles on a piece of nylon membrane (5 cm × 8 cm),
176 and the membrane was dried at 65 °C for 0.5 hour. Probes were prepared in a 40 μL
177 reaction mixture containing 10 U of Klenow enzyme; 25 pmol of biotin-labelled
178 random hexamer primers and 500 ng of template DNA amplified from the introns of
179 45S pre-rRNA. Dot blot hybridization was performed using standard procedures.
180 After hybridization, the membrane was incubated for 1 hour in a 5% skimmed milk-
181 PBS solution containing 1 μL of an anti-biotin HRP-linked antibody and was washed
182 twice with 1×PBS and detected with ECL reagent.

183 *Cell proliferation assays*

184 Cell proliferation assays for HeLa and HepG2 cell lines expressing STAT3 shRNA
185 or mCherry-STAT3 were performed using different approaches, including cell
186 counting, CCK8, EdU and colony formation. Cell counting, CCK-8 and EdU assays
187 were performed as described previously [46, 47]. For colony formation, cell lines
188 expressing STAT3 shRNA or mCherry-STAT3 and their corresponding control cell
189 lines were diluted and seeded in 6-well plates. After culturing for 10 days, cell
190 colonies were fixed and then stained for 15 min with 0.02% crystal violet. After that,
191 cell samples were washed, air-dried and photographed with a camera. The number of
192 total colonies and the sizes of individual colonies were calculated and analysed
193 statistically. For the analysis of cell proliferation and colony formation under the
194 treatment with DMSO, STAT3-In-3 (500 nM), CX-5461 (50 nM), and both STAT3-
195 In-3 (500 nM) and CX-5461 (50 nM), experimental procedures were the same as the
196 assays without drug treatment described above.

197 *Animal models for tumor formation*

198 Sixteen of five-week-old BALB/c female nude mice were obtained from the Vital
199 River Laboratory Animal Technology Co. (Beijing, China). The nude mice inhabited a
200 room under a sterile condition with controlled temperature, humidity and light. After
201 adapting for one week, mice were randomly distributed into two groups (n=8 for each
202 group). Each mouse was subcutaneously injected using 1×10^7 HepG2 cells expressing
203 STAT3 shRNA or control shRNA. After 7 days, growing tumors were measured with
204 a Vernier calliper every 3 days. Tumor volumes were calculated using the formula: $V =$

205 $\frac{\pi}{6} \times \text{length} \times \text{width}^2$. At the end of the sixth week, mice bearing a tumor were

206 euthanized under the Animal Welfare Guideline, and the tumors within the mice were
207 removed, weighed, and photographed. Tumor samples randomly picked from controls
208 or treatments were subjected to hematoxylin and eosin (H&E) staining and
209 immunohistochemistry analysis as described previously [48, 49]. For the tumor
210 formation assays under the treatment with different drugs, 24 nude mice were
211 nurtured for 1 week at a sterilized condition. After that, the mice were subcutaneously
212 injected with 1×10^7 HepG2 cells. Five days later, mice were randomly divided into 4
213 groups (n=6 for each group), which were injected with different drugs, including 100

214 μL 0.9% NaCl, 100 μL STAT3-In-3 (3 mM), 100 μL CX-5461 (3.9 mM) and both of
215 STAT3-In-3 (100 μL , 3 mM) and CX-5461 (100 μL , 3.9 mM). Drug injection was
216 carried out every 2 days until mice were euthanized. Tumor sizes and weight were
217 analyzed as described above. Animal experiments for drug inhibitors were clearly
218 labeled without blinding. Mouse model experiments were approved by the Animal
219 and Medical Ethics Committee in the School of Life Science and Health at Wuhan
220 University of Science and Technology. All animal experiments were conducted
221 according to the Animal Welfare Guidelines (China).

222 *Messenger RNA-seq analysis*

223 HepG2 cell lines expressing STAT3 shRNA or control shRNA were cultured in
224 10-cm dishes in triplicates. At 85% confluence, cells were harvested and total RNA
225 was extracted with a Qiagen RNeasy kit and sent to Frasiergen Gene Information Co.
226 (Wuhan, China) for mRNA-seq analysis. RNA libraries were constructed and loaded
227 on a Novaseq 6000 instrument according to the manufacturer's instructions
228 (Illumina, San Diego, USA). DNA sequencing was performed using a 2 \times 150bp
229 paired-end (PE) configuration and sequence data were obtained by the HiSeq
230 Control Software (HCS) + OLB + GAPipeline-1.6 (Illumina). The raw data
231 containing adapter, PCR primers and other fragments less than 20 bases were
232 trimmed with Trimmomatic (v0.30) so that high-quality clean data were achieved.
233 The clean data were aligned to the human reference genome (Hg38) using software
234 Hisat2 (v2.0.1). Differential expression analysis was performed using the DESeq
235 Bioconductor package. GO-TermFinder was used to identify Gene Ontology (GO)
236 terms that annotate a list of enriched genes where their *P*-values were less than 0.05.
237 Computer codes for the volcano plotting of DEGs and dot plot for pathway
238 enrichment analysis were stored in laboratory computer and are available on request.
239 The upstream analysis for the RNA-seq data was performed by Frasiergen Gene
240 Information Co.

241 *Western blot*

242 HeLa and HepG2 cells including control or treatment cells (knockdown and
243 overexpression) were cultured in 6-well plates. At 90% confluence, cells were
244 harvested and lysed with 200 μL of 1xSDS loading buffer (50 mM Tris-HCl, 2% SDS,
245 0.1% Bromophenol blue, 10% Glycerol, 100mM DTT). After boiling for 10 min at
246 100°C within a heat block, 10 μL samples were used for Western blot analysis using
247 the antibodies against STAT3 (CST#9139, CST, USA), UBF (ab244287, Abcam, UK),
248 TBP (SC-421, Santa Cruz Biotech, USA), TAF1A (SC-393600, Santa Cruz Biotech,
249 USA), RPA34 (CSB-PA004932LA01HU, CUSABio, China) and RPA49 (CSB-
250 PA050039, CUSABio, China).

251 *Reporter assays and chromatin immunoprecipitation assays*

252 Reporter assays were performed as described previously [45] using HeLa or HepG2
253 cell lines expressing STAT3 shRNA and their control cell lines, where the reporter
254 vectors driven by the RPA34 promoter and the β -galactase-expressing vectors were
255 co-transfected into these cell lines. For ChIP assays, HepG2 cells or HepG2 cell lines
256 stably expressing STAT3 shRNA or control shRNA were cultured in 10-cm dishes,
257 fixed with 10 mL 1% formaldehyde-containing PBS solution and harvested for

258 chromatin immunoprecipitation (ChIP) analysis. ChIP assays were performed using
259 the protocol described previously [44] except that antibodies for ChIP assays were
260 replaced. The DNA from each ChIP assay was eluted with 40 μ L ddH₂O after
261 chromatin de-crosslinking and DNA purification, and 1 μ L of ChIP DNA sample was
262 used for a qPCR reaction, where 0.5 ng genomic DNA (0.02% input) acted as a
263 positive control in the assay. Relative enrichment was obtained by calculating the
264 percentage for the relative quantity of promoter DNA from 1/40 ChIP DNA samples
265 in that from 0.02% input.

266 *Pearson' correlation, Kaplan Meier Plotting and Statistical analysis*

267 Pearson correlation analysis between STAT3 and RPA34 expression in normal
268 tissues or clinical cancer samples based on the dataset deposited at The Cancer
269 Genome Atlas (TCGA) was performed using the GEPIA online tool
270 (<http://gepia2.cancer-pku.cn/#index>). Kaplan-Meier Plotting showing the relationship
271 between RPA34 expression levels and survival probability or survival time was
272 performed using the Kaplan-Meier Plotter online tools (www.kmplot.com) and the
273 RNA-seq data of liver hepatocellular carcinomas (LIHC) and kidney renal carcinoma
274 (KIRC) deposited at the TCGA. Violin plots were obtained by Graphpad Prism 8
275 based on the expression data of cancer samples deposited at the TCGA.

276 The experiments in this study, including RT-qPCR, proliferation assays, ChIP
277 assays and reporter assays, were carried out with the samples of three biological
278 replicates or three independent experiments at least. All data generated in the
279 experiments were used for statistical analysis without exclusion. The means, standard
280 deviations (SD) and histograms for the data of cell proliferation, tumor growth, RT-
281 qPCR, luciferase assays, and ChIP assays were calculated with the GraphPad Prism
282 8.0 software. *P* values were obtained by student's *t* test or two-way ANOVA wherever
283 it is appropriate.

284

285 **Results**

286 *STAT3 acts as a positive factor to regulate Pol I-directed transcription*

287 It has been shown that cytoskeletal FLNA silencing can stimulate Pol I-directed
288 transcription [44]. Recently, we performed RNA-seq analysis using FLNA-depleted
289 cell line (SRA accession number: SRP318361,
290 <https://www.ncbi.nlm.nih.gov/Traces/study/?acc=PRJNA726417>) and found that
291 FLNA silencing reduced the expression of both STAT3 mRNA and protein (Fig. S1).
292 In addition, transcription factor STAT3 has been shown to regulate cell proliferation,
293 which is associated with Pol I product levels. Based on this information, we
294 hypothesized that STAT3 maybe is required for the regulation of Pol I-directed
295 transcription. To support this hypothesis, we determined the effect of STAT3
296 expression change on the synthesis of Pol I products in SaOS2 cells. Unexpectedly,
297 STAT3 siRNA transfection reduced Pol I product expression rather than stimulating
298 this process in SaOS2 cells (Fig. S2A and B). Consistent results were obtained when
299 similar assays were performed using HeLa and HepG2 cells (Fig. S2C-F). These

300 results suggest that STAT3 is required for normal transcription directed by Pol I and
301 possibly plays a positive role in this process. This result is opposite to that observed in
302 Fig. S1, where FLNA knockdown reduced the expression of STAT3 (Fig. S1) and
303 stimulated the synthesis of Pol I products (44). To clarify the role of STAT3 in Pol I-
304 dependent transcription, we generated several cell lines (HepG2, HeLa, 293T) stably
305 expressing STAT3 shRNA or control shRNA (Fig. 1A, Fig. S2G and I). However, we
306 failed to get the SaOS2 cell line stably expressing STAT3 shRNA. The reason for this
307 outcome is because SaOS2 cells grew extremely slow and many cells died after
308 STAT3 silencing. Analysis of rRNA expression by RT-qPCR showed that STAT3
309 shRNA stable expression significantly reduced the synthesis of Pol I products (Fig.
310 1B, Fig. S2H and J), indicating that STAT3 expression positively correlates with Pol
311 I-directed transcription.

312 To validate the positive role of STAT3 in Pol I-directed transcription, we prepared
313 several cell lines (HepG2, HeLa, 293T) stably expressing mCherry-STAT3 and
314 analyzed the effect of STAT3 overexpression on rRNA synthesis. Evidently, STAT3
315 overexpression enhanced the synthesis of Pol I products in these cell lines (Fig. 1C
316 and D, Fig. S3A-D). Since 5-ethynyl uridine (EU) can be incorporated into the RNA
317 newly synthesized, we next examined the effect of STAT3 expression alteration on
318 rRNA synthesis by performing EU assays using HeLa and HepG2 cell lines
319 established above. Noticeably, STAT3 silencing reduced nucleolar fluorescence
320 intensity (Fig. 1 E and F, Fig. S2K and L). In contrast, STAT3 overexpression
321 augmented nucleolar fluorescence intensity when compared to control cell lines (Fig.
322 1G and H, Fig. S3E and F). Next, we verified these results using a more direct method
323 (Dot blot). The results from Dot blot assays showed that STAT3 silencing reduced the
324 synthesis of pre-rRNA (Fig. 1I and J). Conversely, STAT3 overexpression enhanced
325 this process (Fig. 1K and L). Collectively, these results indicate that STAT3 plays a
326 positive role in the regulation of Pol I-directed transcription in tumor cells.

327 *Both CRISPR dCas9 activation or repression systems and a STAT3 inhibitor*
328 *confirmed the positive role of STAT3 in Pol-I directed transcription*

329 In order to gain further evidence to support that STAT3 functions as a positive
330 factor in Pol I-mediated transcription, we utilized the CRISPR dCas-9 systems to
331 activate or inhibit endogenous STAT3 expression and observed the effect of STAT3
332 activation or inhibition on rRNA synthesis. We show that endogenous STAT3
333 inhibition dampened the synthesis of Pol I products (Fig. 2A-C), while endogenous
334 STAT3 activation enhanced the expression of Pol I products (Fig. 2D-F). Previous
335 studies showed that STAT3 has to be phosphorylated before entering a nucleus [2];
336 STAT3-IN-3 can impede the phosphorylation of STAT3 at its Tyr⁷⁰⁵ and Ser⁷²⁷ sites
337 [31], which is required for the entry of STAT3 into nuclei. Thus, we determined the
338 effect of STAT3-IN-3 on Pol I-dependent transcription in HeLa or HepG2 cells
339 cultured in the medium containing 5 μmol/L of STAT3-IN-3. Interestingly, the
340 presence of STAT3-IN-3 did not affect STAT3 expression but down-regulated STAT3
341 phosphorylation levels and the synthesis of Pol I products in both HeLa and HepG2
342 cells (Fig. 2G-J), suggesting that STAT3 phosphorylation is required for Pol I-directed
343 transcription. STAT3 and Pol I products have an abnormally high expression in a

344 subset of cancer types [1, 2, 37]. Thus, we next determined whether the expression of
345 STAT3 and Pol I products in HeLa and HepG2 cells is higher than that in their
346 corresponding normal cell lines using Western blot and RT-qPCR techniques. As
347 expected, HeLa and HepG2 cells showed higher levels of STAT3 and Pol I products
348 than their normal cell lines, including HUVEC and HL-7702 cells (Fig 2K and L, Fig.
349 S4). These results further confirmed that STAT3 functions as a positive regulator in
350 Pol I-dependent transcription in human cancer cells.

351 *STAT3 may regulate tumor cell growth in vitro and in vivo by affecting Pol I-directed*
352 *transcription*

353 Because STAT3 expression change affected Pol I product synthesis, and Pol I
354 product levels correlate closely with cell growth [35, 36]; it is necessary to determine
355 the effect of STAT3 upregulation or downregulation on cell proliferation. To this end,
356 the proliferative activity of several cell lines, including HeLa, HepG2 and 293T cell
357 lines with STAT3 depletion or overexpression, was initially analyzed by cell counting
358 and CCK-8 methods. Apparently, STAT3 silencing reduced cell proliferative activity
359 for these cell lines (Fig. 3A and B, Fig. S5A-D). In contrast, STAT3 overexpression
360 enhanced cell proliferative activity (Fig. 3C and D, Fig S6 A-D). The incorporation of
361 5-ethynyl-2'-deoxyuridine (EdU) into genomic DNA is widely utilized to assess the
362 activity of cell proliferation. EdU assays showed that STAT3 downregulation reduced
363 the rate of EdU positive cells, while STAT3 overexpression augmented the rate of
364 EdU-labelled cells (Fig. 3E-H, Fig. S5E and F and Fig. S6E and F). Consistent results
365 were obtained using HepG2 cells with endogenous STAT3 inhibition or activation by
366 a dCas-9 system (Fig. S5G and H, Fig. S6 G and H). To further understand how
367 STAT3 expression alteration affects cancer cell growth, we performed colony
368 formation assays using HepG2 cell lines with STAT3 depletion or overexpression.
369 Analysis of the colony number and size revealed that STAT3 downregulation reduced
370 the number of total colonies and the sizes of individual colonies (Fig. S7A-C), while
371 STAT3 overexpression enhanced them (Fig. S7D-F). These data suggest that STAT3
372 promotes cell growth by reducing cell death and increasing proliferative activity. We
373 showed that STAT3 can concurrently promote cell proliferation and activate Pol I
374 product synthesis. Therefore, we determined whether the increase of Pol I products
375 induced by STAT3 overexpression contributes to the promotion of cell proliferation.
376 Cell proliferation assays were performed in the presence and absence of CX-5461 (a
377 Pol I transcription inhibitor) using HeLa and HepG2 cell lines stably expressing
378 mCherry-STAT3. Strikingly, the presence of CX-5461 inhibited the enhancement of
379 cell proliferation and the activation of Pol I-directed transcription induced by STAT3
380 overexpression (Fig. 3I and J, Fig. S8). These data indicate that the increase of Pol I
381 products contributes to the promotion of cell proliferation induced by STAT3
382 overexpression although the contribution of other pathways cannot be excluded.

383 To understand if alteration of Pol I products by STAT3 silencing affects cell growth
384 *in vivo*, we performed tumor formation assays using nude mice (n=8 for each group)
385 subcutaneously injected with 1×10^7 HepG2 cells stably expressing STAT3 shRNA or
386 control shRNA. Analysis of tumor sizes and weights showed that the tumors with
387 STAT3 silencing showed the reduction in sizes and weights compared to those

388 without STAT3 silencing (Fig. 4A-C). Further assays revealed that tumor tissues
389 formed in nude mice possessed the morphology of liver cancer tissues (Fig. 4D) and
390 retained the original features of HepG2 cells before injection (Fig. 4E-G). These data
391 indicate that STAT3 silencing can inhibit tumour growth *in vivo*, which is associated
392 with the reduction of Pol I products.

393 *The presence of both STAT3-IN-3 and CX-5461 shows additive effect on the*
394 *inhibition of tumour cell growth in vitro and in vivo*

395 STAT3-IN-3 has been reported to suppress breast cancer cell growth [31]. Thus,
396 we next evaluated the effect of STAT3-IN-3 on the proliferative activity of HeLa and
397 HepG2 cells. Notably, the presence of STAT3-IN-3 repressed the proliferative activity
398 of these two cell types (Fig. 5A and B, Fig. S9). Since the presence of CX-5461 (a Pol
399 I-specific inhibitor) suppresses the proliferation activity of HeLa and HepG2 cells
400 (Fig. 3I and J, Fig. S8), we next investigated whether the combination of STAT3-IN-3
401 and CX-5461 can cause greater inhibition to cell proliferation than the application of a
402 single drug. Interestingly, the treatments with both CX-5461 and STAT3-IN-3 showed
403 greater inhibition to HepG2 cell proliferation than the treatments with CX-5461 or
404 STAT3-IN-3 (Fig. 5C and D). Whether the combination of STAT3-IN-3 and other Pol
405 I inhibitors such as actinomycin D and BMH-21 can cause the same effect as
406 observed above is unclear. Thus, HepG2 cells were treated with STAT3-IN-3 and
407 actinomycin D (or BMH-21); and the results confirmed that the treatments with two
408 drugs still showed additive effect on cell growth compared to the treatments with one
409 drug (Fig. S10A-D). Next, we determined how these drugs inhibit cell growth by
410 initially analyzing expression of a cell proliferation marker (CDKN1B) and apoptosis
411 related factors (Caspas-3 and cleaved Caspase-3) in HepG2 cells by Western blot. The
412 treatments with both STAT3-IN-3 and CX-5461 increased expression of CDKN1B
413 and cleaved caspase-3 and reduced expression of Caspase-3; however, the treatments
414 with a single drug had little effect on expression of these proteins (Fig. S10E and F),
415 suggesting that these two drugs may inhibit cell growth by affecting cell proliferation
416 and apoptosis. To verify this result, we performed colony formation assays; and the
417 results showed that all treatments with drugs reduced the number of total colonies and
418 the sizes of individual colonies compared to the DMSO treatment, indicating that both
419 inhibitors can induce cell death and inhibit cell proliferation. Furthermore, the
420 treatments with both CX-5461 and STAT3-IN-3 showed greater inhibition to the
421 number and sizes of colonies than the treatments with a single drug (Fig. 5E-G),
422 indicating that the application of two drugs has additive effect on the inhibition of
423 colony formation.

424 To determine whether these results can be reproduced *in vivo*, we injected HepG2
425 cells into nude mice (n=6 for each group) to allow them form tumors for 5 days. The
426 mice bearing a tumor were treated with different combinations of drugs. Analysis of
427 tumor sizes revealed that the average size of the tumors from the mice treated with
428 drugs was significantly smaller than that from the mice treated with 0.9% NaCl.
429 Furthermore, drug treatments did not affect the weights of mice significantly (Fig. 5H
430 and I). Strikingly, the treatments with both of CX-5461 and STAT3-IN-3 exhibited
431 greater inhibition to tumor volumes and weights compared to the treatments with CX-

432 5461 or STAT3-IN-3 only (Fig. 5H, J and K). Collectively, these data indicate that the
433 application of both CX-5461 and STAT3-IN-3 has additive effect on the suppression
434 of HepG2 cell growth *in vitro* and *in vivo* compared to the application of CX-5461 or
435 STAT3-IN-3.

436 *Messenger RNA-seq revealed the regulation of RPA34 expression by STAT3*

437 To understand how STAT3 regulates Pol I-directed transcription, we first
438 determined whether STAT3 can be localized to the nucleoli of human cells.
439 Immunofluorescence (IF) assays were performed using HeLa and HepG2 cells and
440 the antibodies against STAT3 or Fibrillarlin (a nucleolar protein marker).
441 Unexpectedly, STAT3 couldn't be observed in the nucleoli of these cells (Fig. S11),
442 suggesting that STAT3 indirectly regulates Pol I-mediated transcription. To gain a clue
443 about how STAT3 modulates Pol I-directed transcription, we performed RNA-seq
444 analysis using the total RNA extracted from HepG2 cell lines stably expressing
445 STAT3 shRNA or control shRNA. RNA-seq analysis showed that STAT3 silencing
446 caused expression downregulation of 1223 genes and expression upregulation of 931
447 genes (Fig. 6A). Analysis of gene ontology (GO) and pathways revealed that
448 significant differential expression genes (DEGs) induced by STAT3 silencing in
449 HepG2 cells contain ribosome-related GO terms or pathways (Fig. S12A and B),
450 indicating that STAT3 expression is associated with ribosome pathway. Indeed, Pol I
451 product alteration has been shown to affect ribosome biogenesis [35, 36].
452 Unexpectedly, among significant DEGs (\log_2 fold change > 0.6), the genes encoding
453 any of the Pol I transcription machinery factors couldn't be found. Next, we examined
454 all expression dataset by removing the threshold of significant difference.
455 Consequently, the expression of three genes encoding Pol I machinery factors such as
456 RPA12, RPA34 and TAF1C showed reasonable reduction after STAT3 silencing (Fig.
457 6B). RT-qPCR confirmed that RPA34 mRNA expression was affected by both STAT3
458 silencing and overexpression in both HeLa and HepG2 cells, whereas alteration of
459 RPA12 and TAF1C expression showed inconsistency between HeLa and HepG2 cell
460 lines or between STAT3 depletion and overexpression (Fig. 6C-F). Western blotting
461 confirmed that STAT3 silencing reduced RPA34 protein expression in both HepG2
462 and HeLa cells, whereas TAF1C expression was not affected by STAT3 knockdown in
463 both cell types. Unexpectedly, RPA12 expression was affected by STAT3 silencing in
464 HepG2 cells but not in HeLa cells (Fig. 6G and H). Since RPA34 is usually located in
465 the nucleoli of human cells, we next examined whether alteration of STAT3
466 expression affects RPA34 levels in the nucleoli by performing immunofluorescence
467 (IF) staining. IF data showed that STAT3 silencing reduced the RPA34 levels in the
468 nucleoli of HepG2 cells compared to the control cell line (Fig. S13). Taken together,
469 these results indicate that STAT3 can positively regulate RPA34 expression at both
470 RNA and protein levels in HepG2 and HeLa cells.

471 *Cancer patients with RPA34 abnormal high expression lead to low survival*
472 *probability*

473 The results obtained above (Fig. 6) suggest a positive regulatory relationship
474 between STAT3 and RPA34. To further confirm this observation, we performed the
475 analysis of Pearson correlation between STAT3 and RPA34 based on the RNA-seq

476 data of cancer samples deposited at The Cancer Genome Atlas (TCGA). Interestingly,
477 positive correlation between STAT3 and RPA34 expression was observed in several
478 cancer types, including liver hepatocellular carcinoma (LIHC, R=0.3), kidney renal
479 clear cell carcinoma (KIRC, R=0.5), kidney renal papillary cell carcinoma (KIRP,
480 R=0.65), thymoma (THYM, R=0.77), diffuse large B-cell lymphoma (DLBC,
481 R=0.69) and thyroid carcinoma (THCA, R=0.63) (Fig. 7A-C, Fig. S14). Further,
482 strong positive correlation (R=0.79) between STAT3 and RPA34 expression was also
483 observed in normal tissues when Pearson correlation analysis was performed using
484 the RNA-seq data of liver, cervix and kidney tissues deposited at the TCGA (Fig. 7D).
485 Next, we analyzed the expression difference of RPA34 between cancer cells and
486 normal cells by Western blot. Clearly, both HeLa and HepG2 cells have higher RPA34
487 expression than their normal cell lines, HUVEC and HL-7702, respectively (Fig.
488 S15A and B). Interestingly, the presence of STAT3-IN-3 dampened RPA34 expression
489 in both HeLa and HepG2 cells (Fig.S15C and D). We next determined whether the
490 expression difference of RPA34 between cancer and normal tissues is similar to that
491 between tumor and normal cell lines. Thus, RPA34 expression was analyzed based on
492 the RNA-seq data in the TCGA database, and the results were presented in Fig 7E and
493 F. Apparently, both liver hepatocellular carcinomas (LIHC) and kidney renal
494 carcinomas (KIRC) showed higher RPA34 expression than their normal tissues. We
495 then addressed whether high levels of RPA34 expression can affect cancer patient
496 survival rate. To this end, we performed Kaplan-Meier plotting using the RNA-seq
497 dataset of liver hepatocellular carcinomas (LIHC) and kidney renal carcinoma (KIRC)
498 obtained from the TCGA database. We showed that the patients with RPA34 high
499 expression levels in liver hepatocellular carcinomas (LIHC) or kidney renal
500 carcinomas (KIRC) exhibited lower survival probability and shorter survival time
501 when compared to the patients with low RPA34 expression levels. Taken together,
502 cancer patients with high levels of RPA34 expression may lead to low survival rate,
503 suggesting that RPA34 may act as a biomarker of poor prognosis in a subset of
504 cancers.

505 *STAT3 modulates the recruitment of the Pol I transcription machinery components to*
506 *the rDNA promoter by controlling RPA34 expression*

507 Apart from RPA34, whether alteration of STAT3 expression affects the expression
508 of other factors related to Pol I transcription at the protein level is unclear. Thus, we
509 analyzed the expression of a few factors related to Pol I transcription apparatus by
510 Western blot using cell lines with STAT3 silencing or overexpression.
511 Immunoblotting results showed that both STAT3 upregulation and downregulation
512 affected RPA34 expression in HeLa and HepG2 cells. However, the expression of
513 UBF, TAF1A, and RPA49 was variable between two cell types or between STAT3
514 knockdown and overexpression samples (Fig. 8A-D, Fig. S16). Since STAT3
515 positively regulates the synthesis of Pol I products, we determined whether STAT3
516 binds to the rDNA promoter by performing ChIP assays. ChIP qPCR data showed
517 that STAT3 does not bind to the rDNA promoter (Fig. 8E). This result is consistent
518 with that obtained in IF assays (Fig. S11). We next investigated whether alteration of
519 STAT3 expression affects the assembly of the Pol I transcription machinery factors

520 at the rDNA promoter by performing ChIP assays using HepG2 cells. We showed
521 that STAT3 silencing reduced the occupancies of the Pol I transcription machinery
522 factors at the rDNA promoter, while STAT3 overexpression enhanced the
523 occupancies of these factors at the promoter (Fig. 8F and G), suggesting that STAT3
524 can modulate the recruitment of the Pol I transcription machinery factors to the
525 rDNA promoter by affecting RPA34 expression. Next, we addressed whether
526 alteration of STAT3 expression can affect the rDNA promoter (rDNAP) activity. To
527 achieve this goal, we amplified the rDNA promoter along with the DNA fragment
528 encoding about 300 nt 45S pre-rRNA immediately downstream of the promoter, the
529 resulting DNA was inserted into the pGL3-basic. The promoter-driven reporter
530 vectors were transfected into HeLa and HepG2 cell lines. RT-qPCR was used to
531 detect the expression of a 'reporter' gene using the primers as indicated in Fig. 8H.
532 The results showed that STAT3 knockdown inhibited the rDNAP activity; whereas
533 STAT3 overexpression activated the rDNAP activity in both of cell types (Fig. 8I-L).
534 Collectively, these data indicate that STAT3 can modulate the recruitment of
535 components of the Pol I transcription machinery to the rDNA promoter by
536 controlling RPA34 expression, which consequently affects the transcription activity
537 of the rDNA promoter.

538 *STAT3 regulates Rpa34 gene transcription by binding to the Rpa34 promoter*

539 To determine whether RPA34 is required for the regulation of Pol I transcription
540 mediated by STAT3, we performed rescue experiments by expressing mCherry-
541 RPA34 in HepG2 and HeLa cell lines with STAT3 depletion. The results from the
542 rescue experiments showed that mCherry-RPA34 expression reversed the inhibition of
543 Pol I-directed transcription induced by the STAT3 silencing (Fig. 9A and B, Fig. S17
544 A and B) and alleviate the repression of HepG2 cell growth caused by STAT3
545 silencing (Fig. 9C and D, Fig. S17 C and D), indicating that RPA34 participates in the
546 regulation of Pol I-directed transcription mediated by STAT3. We then determined
547 whether RPA34 expression alteration affects the synthesis of Pol I products by in
548 HepG2 and HeLa cells using a lentiviral expression system. We showed that RPA34
549 silencing reduced the synthesis of Pol I products (Fig. 9E and F, Fig. S17 E and F). In
550 contrast, RPA34 overexpression increased Pol I product expression (Fig. 9G and H,
551 Fig. S17 G and H), indicating RPA34 positively regulates the synthesis of Pol I
552 products. To understand how STAT3 regulates RPA34 expression, we searched for the
553 STAT3-binding motif in the *Rpa34* gene promoter. Surprisingly, the *Rpa34* promoter
554 contains two putative STAT3 consensus sequences upstream of the transcription start
555 site (Fig. 9I). ChIP assays confirmed that STAT3 can bind to the *Rpa34* promoter (Fig.
556 9J). Next, the *Rpa34* promoter was inserted into the pGL3-basic reporter vector and
557 the *Rpa34* promoter activity was examined by performing luciferase assays. We
558 showed that STAT3 silencing reduced the *Rpa34* promoter activity, while STAT3
559 overexpression enhanced its activity (Fig. 9K and L, Fig. S17I and J). Mutations of
560 STAT3 binding sites blunted the activity of the *Rpa34* promoter (Fig. 9M and N),
561 indicating that STAT3 controls *Rpa34* gene expression at the transcription step. To
562 understand how STAT3 regulates *Rpa34* gene transcription, we performed ChIP
563 assays using HepG2 cell lines expressing STAT3 shRNA or control shRNA. ChIP-

564 qPCR showed that STAT3 silencing inhibited the assembly of the RNA polymerase II
565 transcription machinery factors at the *Rpa34* promoter (Fig. 9O). These data suggest
566 that STAT3 regulates *Rpa34* gene transcription by affecting the recruitment of Pol II
567 transcription machinery factors to the *Rpa34* promoter.

568 Based on the data obtained in this study, we proposed a model by which STAT3
569 regulates Pol I-directed transcription. Specifically, after phosphorylation, STAT3
570 enters nuclei and directly binds to the *Rpa34* promoter to modulate *Rpa34* gene
571 transcription. After translation in cytoplasm, RPA34 enters the nucleoli of human cells
572 and binds to the rDNA promoter along with other factors of the Pol I transcription
573 machinery. Consequently, STAT3 modulates Pol I-directed transcription by
574 controlling RPA34 expression and the assembly of the Pol I transcription machinery
575 at the rDNA promoter (Fig. 10).

576 Discussion

577 Previous studies showed that STAT3 can be activated by canonical signaling
578 pathways. Upon activation, STAT3 is phosphorylated and forms a homodimer to
579 enter the nucleus, where phosphorylated STAT3 regulates the transcription of target
580 genes directed by RNA polymerase II [1, 2]. In this study, however, we found that
581 STAT3 can positively regulate 45S ribosomal RNA expression. Thus, we identified a
582 novel role of STAT3 in transcriptional regulation in this work. This finding seems
583 contradiction with the initial observation in FLNA-depleted SaOS2 cells, where
584 FLNA silencing reduced STAT3 expression (Fig. S1) but increased expression of Pol
585 I products [44]. This discrepancy may be because thousands of differential
586 expression genes were downregulation and upregulation in FLNA-depleted SaOS2
587 cells [50], and STAT3 might not play a key role in this situation; instead, FLNA acts
588 as a key regulator in Pol I-directed transcription and regulates it by a sequestration
589 mode [44]. In recent years, many novel factors, including non-coding RNA and
590 proteins, have been shown to regulate cancer development by affecting STAT3
591 signaling [3, 25, 51, 52]. Thus, the function of STAT3 identified in this study extends
592 the understanding of the regulatory mechanism of gene transcription and cancer
593 development mediated by STAT3. We showed that STAT3 can activate RPA34
594 expression but not expression of Pol I general transcription factors (Fig. 6, Fig. 8),
595 and STAT3 enhances the recruitment of the Pol I transcription machinery to the
596 rDNA promoter by increasing RPA34 expression (Fig. 8). Furthermore, STAT3
597 activates *Rpa34* gene transcription by binding to the *Rpa34* promoter, and RPA34
598 silencing affected the synthesis of Pol I products [Fig. 9], indicating that STAT3
599 regulates Pol I-dependent transcription by controlling RPA34 expression, This result
600 is distinct from the previous findings in which the oncogenic factor MYC regulates
601 Pol I-dependent transcription by interacting with the ribosomal DNA promoter rather
602 than Pol I subunit [39, 53]. This study provides a novel mechanism by which the
603 oncogenic factor STAT3 modulate Pol I-dependent transcription

604 STAT3 has become an appealing target for anti-cancer therapy due to its activating
605 role in cancer development for a subset of cancers [1, 3]. In this work, we found that
606 STAT3 has higher expression in HeLa and HepG2 cells than it does in normal cells,

607 and STAT3 promotes proliferation activity for these cell types. Additionally, abnormal
608 high expression of its downstream factor RPA34 in a subset of cancers was observed,
609 and cancer patients with high expression of RPA34 have lower survival rate and
610 shorter survival time compared those with low expression of RPA34 (Fig 7). These
611 data suggest that STAT3 may modulate cancer development by influencing the
612 expression of its downstream factor RPA34, and RPA34 can act as a biomarker of
613 poor prognosis in subset of cancer types. Intriguingly, the presence of STAT3-IN-3
614 can severely inhibit cell proliferation and induce cell death (Figs. 2, 3 and 5; Figs. S4-
615 8, Fig. S10). Additionally, the Pol I-specific inhibitor CX5461 represses proliferation
616 activity for these cell types by inhibiting the increase of Pol I products induced by
617 STAT3 overexpression (Fig. 3I and J). These results suggest that tumor cell growth
618 can be concurrently inhibited by STAT3-IN-3 and CX-5461. Indeed, the tumor cells
619 treated with both STAT3-IN-3 and CX-5461 (or BMH-21/Actinomycin D) led to
620 additive effect on cancer cell deaths or cell growth suppression *in vitro* and *in vivo*
621 when compared to the cells were treated with either of the inhibitors (Fig. 5, Fig.
622 S10A-D). Currently, multiple drugs are often used for anti-cancer research as well as
623 cancer therapy in the clinic [54, 55]. Thus, the result of inhibitor assays has profound
624 medical significance because STAT3-IN-3 and Pol I transcription inhibitors would act
625 as combined drugs in cancer therapy in the future.

626 **Conclusions**

627 In this study, we identified a positive role of STAT3 in Pol I-directed transcription
628 in human tumor cells. STAT3 positively regulates cancer cell survival and growth *in*
629 *vitro* and *in vivo*. The presence of both of STAT3 and Pol I transcription inhibitors has
630 a greater inhibitory effect on tumor cell growth than the application of either
631 inhibitors. STAT3 activates RPA34 transcription by binding to the *Rpa34* promoter,
632 which consequently controls Pol I-directed transcription by affecting the Pol I
633 transcription machinery assembly at the rDNA promoter. RPA34 has s abnormal high
634 expression in subset of cancer types, and cancer patients with RPA34 high expression
635 exhibits poor prognosis. Our findings provide a novel insight into Pol I-directed
636 transcription and a promising prospect that STAT3 and Pol I-specific inhibitors may
637 act as combined drugs in cancer therapy.

638 **Abbreviations**

639 STAT3, signal transducer and activator of transcription 3; Pol I, RNA Polymerase I;
640 Pol II, RNA polymerase II; RPA34, DNA-directed RNA Polymerase I subunit RPA34;
641 EU, 5-ethynyl uridine; EdU, 5-ethynyl-2'-deoxyuridine, p-STAT3, phosphorylated
642 STAT3; mCherry-STAT3, mCherry-tagged STAT3 fusion protein; GAPDH,
643 glyceraldehyde-3-phosphate dehydrogenase; TBP, TATA box-binding protein;
644 RPA40, DNA-directed RNA polymerase I subunit RPA40; UBF, upstream binding
645 factor; TAF1A, TBP-associated factor 1A; RPA49, DNA-directed RNA polymerase I
646 subunit RPA49; FLNA, Filamin A; STAT3-IN-3, STAT3 inhibitor 3; CX-5461, 2-(4-
647 methyl-1,4-diazepan-1-yl)-N-[(5-methylpyrazin-2-yl)methyl]-5-oxo-
648 [1,3]benzothiazolo[3,2-a][1,8]naphthyridine-6-carboxamide (Pol I-mediated rRNA

649 synthesis inhibitor), BMH-21 (Pol I elongation inhibitor), N-[2-
650 (dimethylamino)ethyl]-12-oxo-12H-benzo[g]pyrido[2,1-b]quinazoline-4-
651 carboxamide.

652 **Additional Information**

653 **Acknowledgements**

654 Not applicable.

655 **Authors' contributions:**

656 CZ performed most work in Figures 1-8 and in the supplementary file; JW validated
657 data and mentored researchers; YS and DY performed cell culture and cell line
658 screening; YP and BG performed gene cloning; HD prepared CRPSR dCas9
659 expression system, designed experiments and performed a part of supervision work;
660 XY performed RPA34 shRNA cloning; S Zhang and S Zhao performed most of the
661 supervision work, processed data, and edited the manuscript; WD acquired the fund of
662 this work, designed experiments, processed data, and wrote the manuscript.

663 **Ethics approval and consent to participate**

664 Animal experiments were approved by the Animal and Medical Ethics Committee
665 of School of Life Science and Health at Wuhan University of Science and
666 Technology. The animal protocols abided by the Animal Welfare Guidelines (China).

667 **Consent for publication**

668 Not applicable.

669 **Data availability**

670 The RNA-seq data about SaOS2 cell FLNA silencing were deposited in the NCBI
671 repository (SRA: SRP318361,
672 <https://www.ncbi.nlm.nih.gov/Traces/study/?acc=PRJNA726417>). The RNA-seq data
673 about HepG2 cell STAT3 silencing were deposited in the NCBI Gene Expression
674 Omnibus (GSE201548,
675 <https://www.ncbi.nlm.nih.gov/geo/query/acc.cgi?acc=GSE201548>). The RNA-seq
676 data used for Pearson correlation analysis, Kaplan Meier plotting and Violin plotting
677 were obtained from the TCGA database (www.tcgaportal.org).

678 **Competing interests**

679 The authors declare no potential conflicts of interest.

680 **Funding information**

681 This work was funded by the National Natural Science Foundation of China
682 (31671357 to WD, 62172312 to S Zhang).

683

684

685 **References**

- 686 1. Lee H, Jeong AJ, Ye SK. Highlighted STAT3 as a potential drug target for cancer
687 therapy. BMB Rep. 2019;52:415-423
- 688 2. Srivastava J, DiGiovanni J. Non-Canonical Stat3 Signaling in Cancer. Mol

- 689 Carcinog. 2016;55:1889–1898
- 690 3. Yang L, Lin S, Xu L, Lin J, Zhao C, Huang X. Novel activators and small-
691 molecule inhibitors of STAT3 in cancer. *Cytokine Growth Factor Rev.*
692 2019;49:10–22
- 693 4. Johnson DE, O’Keefe RA, Grandis JR. Targeting the IL-6/JAK/STAT3 signaling
694 axis in cancer. *Nat Rev Clin Oncol.* 2018;15:234-248
- 695 5. Chua CY, Liu Y, Granberg KJ, Hu L, Haapasalo H, Annala MJ, et al. IGFBP2
696 potentiates nuclear EGFR-STAT3 signaling. *Oncogene.* 2016;35:738-747.
- 697 6. Bromberg JF, Wrzeszczynska MH, Devgan G, Zhao Y, Pestell RG, Albanese C,
698 et al. Stat3 as an oncogene. *Cell.* 1999;98:295-303
- 699 7. Aryappalli P, Shabbiri K, Masad RJ, Al-Marri RH, Haneefa SM, Mohamed YA,
700 et al. Inhibition of tyrosine-phosphorylated STAT3 in human breast and lung
701 cancer cells by manuka honey is mediated by selective antagonism of the IL-6
702 receptor. *Int J Mol Sci.* 2019;20:4340
- 703 8. Zhang Q, Raje V, Yakovlev VA, Yacoub A, Szczepanek K, Meier J, et al. Stat3
704 promotes breast cancer growth via phosphorylation of serine 727. *J Biol Chem.*
705 2013;288:31280–31288.
- 706 9. Wegrzyn J, Potla R, Chwae YJ, Sepuri NB, Zhang Q, Koeck T, et al. Function of
707 mitochondrial Stat3 in cellular respiration. *Science.* 2009;323:793–797.
- 708 10. Gough DJ, Corlett A, Schlessinger K, Wegrzyn J, Larner AC, Levy DE.
709 Mitochondrial STAT3 supports Ras-dependent oncogenic transformation.
710 *Science.* 2009;324:1713–1716.
- 711 11. Macias E, Rao D, Carbajal S, Kiguchi K, Digiovanni J. Stat3 binds to mtDNA
712 and regulates mitochondrial gene expression in keratinocytes. *J Invest Dermatol.*
713 2014;134:1971-1980.
- 714 12. Tammineni P, Anugula C, Mohammed F, Anjaneyulu M, Larner AC, Sepuri NB.
715 The import of the transcription factor STAT3 into mitochondria depends on
716 GRIM-19, a component of the electron transport chain. *J Biol Chem.*
717 2013;288:4723–4732
- 718 13. Braunstein J, Brutsaert S, Olson R, Schindler C. STATs dimerize in the absence
719 of phosphorylation. *J Biol Chem.* 2003;278:34133–34140.
- 720 14. Yang JB, Stark GR. Roles of unphosphorylated STATs in signaling. *Cell*
721 *Research.* 2008;18:443–451
- 722 15. Yang J, Liao X, Agarwal MK, Barnes L, Auron PE, Stark GR. Unphosphorylated
723 STAT3 accumulates in response to IL-6 and activates transcription by binding to
724 NFkappaB. *Genes Dev.* 2007;21:1396–1408
- 725 16. Yang J, Chatterjee-Kishore M, Staugaitis SM, Nguyen H, Schlessinger K, Levy
726 DE, et al. Novel roles of unphosphorylated STAT3 in oncogenesis and
727 transcriptional regulation. *Cancer Res.* 2005;65:939–947.
- 728 17. Zhao J, Du P, Cui P, Qin Y, Hu C, Wu J, et al. LncRNA PVT1 promotes
729 angiogenesis via activating the STAT3/VEGFA axis in gastric cancer. *Oncogene.*
730 2018;37:4094–4109

- 731 18. Huang Z, Zhou W, Li Y, Cao M, Wang T, Ma Y, et al. Novel hybrid molecule
732 overcomes the limited response of solid tumors to HDAC inhibitors via
733 suppressing JAK1-STAT3-BCL2 signalling. *Theranostics*. 2018;8:4995–5011
- 734 19. Su K, Zhao Q, Bian A, Wang C, Cai Y, Zhang Y. A novel positive feedback
735 regulation between long noncoding RNA UICC and IL-6/STAT3 signaling
736 promotes cervical cancer progression. *Am J Cancer Res*. 2018;8:1176–1189
- 737 20. Dai W, Liu S, Zhang J, Pei M, Xiao Y, Li J, et al. Vorinostat triggers miR-769-
738 5p/3p-mediated suppression of proliferation and induces apoptosis via
739 the STAT3-IGF1R-HDAC3 complex in human gastric cancer. *Cancer Lett*.
740 2021;S0304-3835(21)00437-7.
- 741 21. Chuang CH, Greenside PG, Rogers ZN, Brady JJ, Yang D, Ma RK, et al.
742 Molecular definition of a metastatic lung cancer state reveals a targetable CD109-
743 Janus kinase-Stat axis. *Nat Med*. 2017;23:291–300
- 744 22. Jia L, Wang Y, Wang CY. circFAT1 promotes cancer stemness and immune
745 evasion by promoting STAT3 activation. *Adv Sci (Weinh)*. 2021;8(13):2003376
- 746 23. Cayrol F, Praditsuktavorn P, Fernando TM, Kwiatkowski N, Marullo R, Calvo-
747 Vidal MN, et al. THZ1 targeting CDK7 suppresses STAT transcriptional activity
748 and sensitizes T-cell lymphomas to BCL2 inhibitors, *Nat Commun*. 2017;8:14290
- 749 24. He L, Pratt H, Gao M, Wei F, Weng Z, Struhl K. YAP and TAZ are transcriptional
750 co-activators of AP-1 proteins and STAT3 during breast cellular transformation.
751 *Elife*. 2021;10:e67312.
- 752 25. Lv D, Li Y, Zhang W, Alvarez AA, Song L, Tang J, et al. TRIM24 is an
753 oncogenic transcriptional co-activator of STAT3 in glioblastoma. *Nat Commun*.
754 2017;8:1454.
- 755 26. Wang ST, Ho HJ, Lin JT, Shieh JJ, Wu CY. Simvastatin-induced cell cycle arrest
756 through inhibition of STAT3/SKP2 axis and activation of AMPK to promote p27
757 and p21 accumulation in hepatocellular carcinoma cells. *Cell Death Dis*.
758 2017;8:e2626
- 759 27. Chung SS, Adekoya D, Enenmoh I, Clarke O, Wang P, Sarkyssian M, et al.
760 Salinomycin abolished STAT3 and STAT1 interactions and reduced telomerase
761 activity in colorectal cancer cells. *Anticancer Res*. 2017;37:445–453
- 762 28. Ahn KS, Sethi G, Sung B, Goel A, Ralhan R, Aggarwal BB. Guggulsterone, a
763 farnesoid X receptor antagonist, inhibits constitutive and inducible STAT3
764 activation through induction of a protein tyrosine phosphatase SHP-1. *Cancer*
765 *Res*. 2008;68:4406–4415
- 766 29. Song JM, Qian X, Upadhyayya P, Hong KH, Kassie F.
767 Dimethylaminoparthenolide, a water soluble parthenolide, suppresses lung
768 tumorigenesis through down-regulating the STAT3 signaling pathway. *Curr*
769 *Cancer Drug Targets*. 2014;14:59–69.
- 770 30. Bai L, Zhou H, Xu R, Zhao Y, Chinnaswamy K, McEachern D, et al. A potent
771 and selective small-molecule degrader of STAT3 achieves complete tumor
772 regression *in vivo*. *Cancer Cell*. 2019; 36:498-511.

- 773 31. Cai G, Yu W, Song D, Zhang W, Guo J, Zhu J, et al. Discovery of fluorescent
774 coumarin-benzo thiophene 1, 1-dioxide conjugates as mitochondria-targeting
775 antitumor STAT3 inhibitors. *Eur J Med Chem.* 2019;174:236-251.
- 776 32. Zhang N, Zhang M, Wang Z, Gao W, Sun ZG. Activated STAT3 could reduce
777 survival in patients with esophageal squamous cell carcinoma by up-
778 regulating VEGF and cyclin D1 expression. *J Cancer.* 2020;11:1859-1868
- 779 33. Bowman T, Broome MA, Sinibaldi D, Wharton W, Pledger WJ, Sedivy JM, et al.
780 Stat3-mediated Myc expression is required for Src transformation and PDGF-
781 induced mitogenesis. *Proc Natl Acad Sci U S A.* 2001;98(13):7319-24.
- 782 34. Gritsko T, Williams A, Turkson J, Kaneko S, Bowman T, Huang M, et al.
783 Persistent activation of stat3 signaling induces survivin gene expression and
784 confers resistance to apoptosis in human breast cancer cells. *Clin Cancer Res.*
785 2006;12:11-9.
- 786 35. Drygin D, Rice WG, Grummt I. The RNA polymerase I transcription machinery:
787 an emerging target for the treatment of cancer. *Annu Rev Pharmacol Toxicol.*
788 2010;50:131-56.
- 789 36. Sharifi S, Bierhoff H. Regulation of RNA Polymerase I Transcription in
790 Development, Disease, and Aging. *Annu Rev Biochem.* 2018;87:5 1–73
- 791 37. Ferreira R, Schneekloth JS Jr, Panov KI, Hannan KM, Hannan RD. Targeting
792 the RNA polymerase I transcription for cancer therapy comes of age. *Cells.*
793 2020;9:266.
- 794 38. Goodfellow SJ, Zomerdijk JC. Basic mechanism in RNA polymerase
795 I transcription of ribosomal RNA genes. *Subcell Biochem.* 2013;61:211-236.
- 796 39. Arabi A, Wu S, Ridderstråle K, Bierhoff H, Shiue C, Fatyol K, et al. c-
797 Myc associates with ribosomal DNA and activates RNA polymerase
798 I transcription. *Nat Cell Biol.* 2005;7:303-10.
- 799 40. Bywater MJ, Poortinga G, Sanij E, Hein N, Peck A, Cullinane C, et al. Inhibition
800 of RNA polymerase I as a therapeutic strategy to promote cancer-specific
801 activation of p53. *Cancer Cell.* 2012;22:51-65.
- 802 41. Mayer C, Bierhoff H, Grummt I. The nucleolus as a stress sensor: JNK2
803 inactivates the transcription factor TIF-IA and down-regulates rRNA synthesis.
804 *Genes Dev.* 2005 Apr 15;19(8):933-41.
- 805 42. Tessarz P, Santos-Rosa H, Robson SC, Sylvestersen KB, Nelson CJ, Nielsen ML,
806 et al. Glutamine methylation in histone H2A is an RNA-polymerase-I-dedicated
807 modification. *Nature.* 2014;505:564-568.
- 808 43. Xing YH, Yao RW, Zhang Y, Guo CJ, Jiang S, Xu G, et al. SLERT regulates
809 DDX21 rings associated with Pol I transcription. *Cell.* 2017;169:664-678
- 810 44. Deng W, Lopez-Camacho C, Tang JY, Mendoza-Villanueva D, Maya-Mendoza A,
811 Jackson DA, et al. Cytoskeletal protein filamin A is a nucleolar protein that
812 suppresses ribosomal RNA gene transcription. *Proc Natl Acad Sci U S A.*
813 2012;109:1524-9
- 814 45. Wang J, Zhao S, Wei Y, Zhou Y, Shore P, Deng W. Cytoskeletal filamin A
815 differentially modulates RNA polymerase III gene transcription in transformed
816 cell lines. *J Biol Chem.* 2016;291:25239-25246.

- 817 46. Peng F, Zhou Y, Wang J, Guo B, Wei Y, Deng H, et al. The transcription factor
818 Sp1 modulates RNA polymerase III gene transcription by controlling BRF1 and
819 GTF3C2 expression in human cells. *J Biol Chem.* 2020;295:4617-4630.
- 820 47. Yin X, Zhang K, Wang J, Zhou X, Zhang C, Song X, et al. RNA polymerase I
821 subunit 12 plays opposite roles in cell proliferation and migration. *Biochem*
822 *Biophys Res Commun.* 2021;560:112-118.
- 823 48. Cardiff RD, Miller CH, Munn RJ. Manual hematoxylin and eosin staining of
824 mouse tissue sections. *Cold Spring Harb Protoc.* 2014;2014:655-658.
- 825 49. Canene-Adams K. Preparation of formalin-fixed paraffin-embedded tissue for
826 immunochemistry. *Methods Enzymol.* 2013;33:225-233.
- 827 50. Zhang C, Zhao H, Song X, Wang J, Zhao S, Deng H, et al. Transcription
828 factor GATA4 drives RNA polymerase III-directed transcription and
829 transformed cell proliferation through a filamin A/GATA4/SP1 pathway. *J Biol*
830 *Chem.* 2022;298:101581.
- 831 51. Bian Z, Ji W, Xu B, Huo Z, Huang H, Huang J, et al. Noncoding RNAs involved
832 in the STAT3 pathway in glioma. *Cancer Cell Int.* 2021;21:445
- 833 52. Filppu P, Tanjore Ramanathan J, Granberg KJ, Gucciardo E, Haapasalo H, Lehti
834 K, et al. CD109-GP130 interaction drives glioblastoma stem cell plasticity and
835 chemoresistance through STAT3 activity. *JCI Insight.* 2021;6:e141486
- 836 53. White RJ. RNA polymerases I and III, non-coding RNAs and cancer. *Trends*
837 *Genet.* 2008;24:622-629.
- 838 54. Szakács G, Paterson JK, Ludwig JA, Booth-Genthe C, Gottesman MM.
839 Targeting multidrug resistance in cancer. *Nat Rev Drug Discov.* 2006;5:219-234.
- 840 55. Unsoy G, Gunduz U. Smart drug delivery systems in cancer therapy. *Curr Drug*
841 *Targets.* 2018;19:202-212.

842

843

844

845

846

847

848

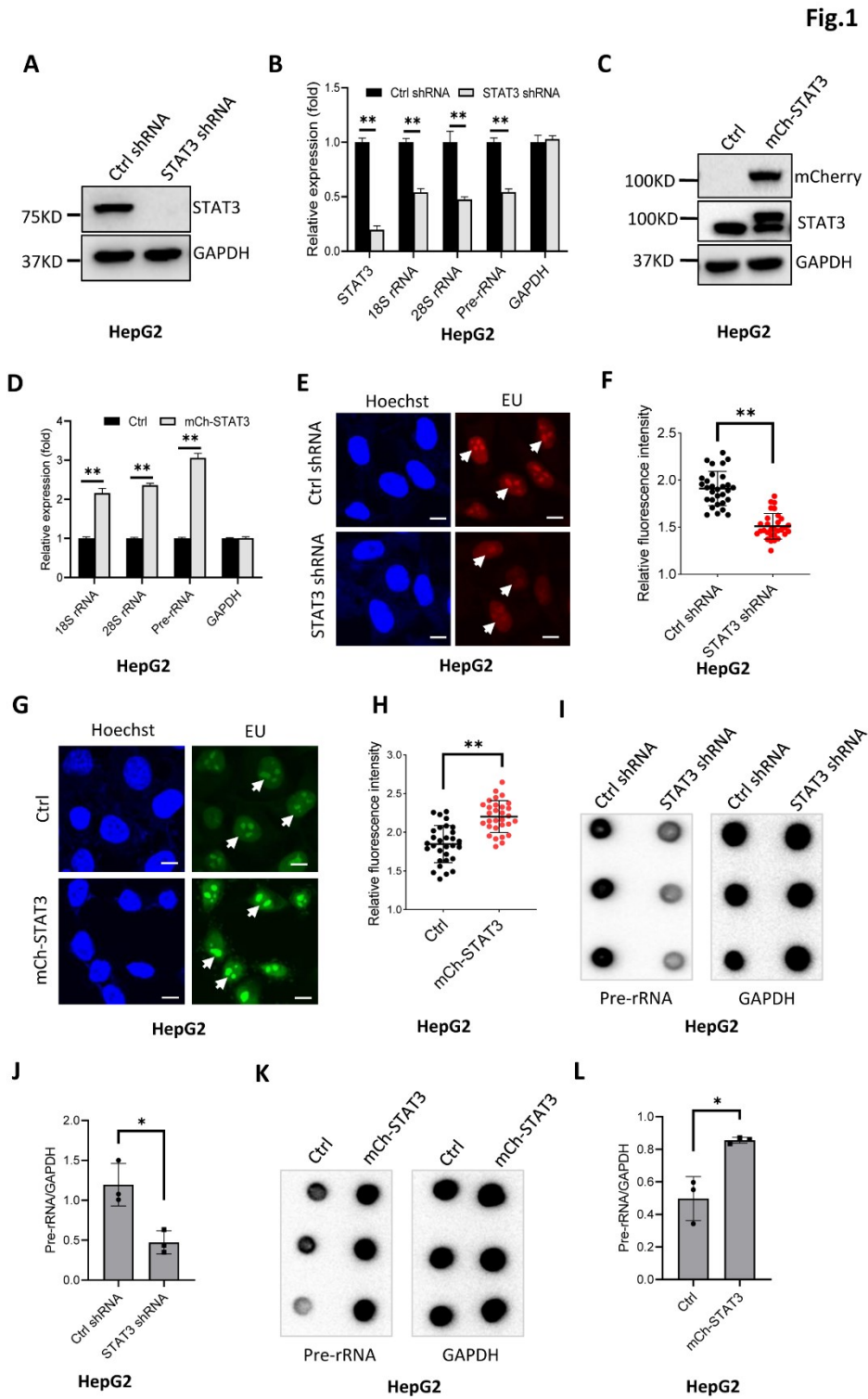
849

850

851

852

853 **Figure legends**



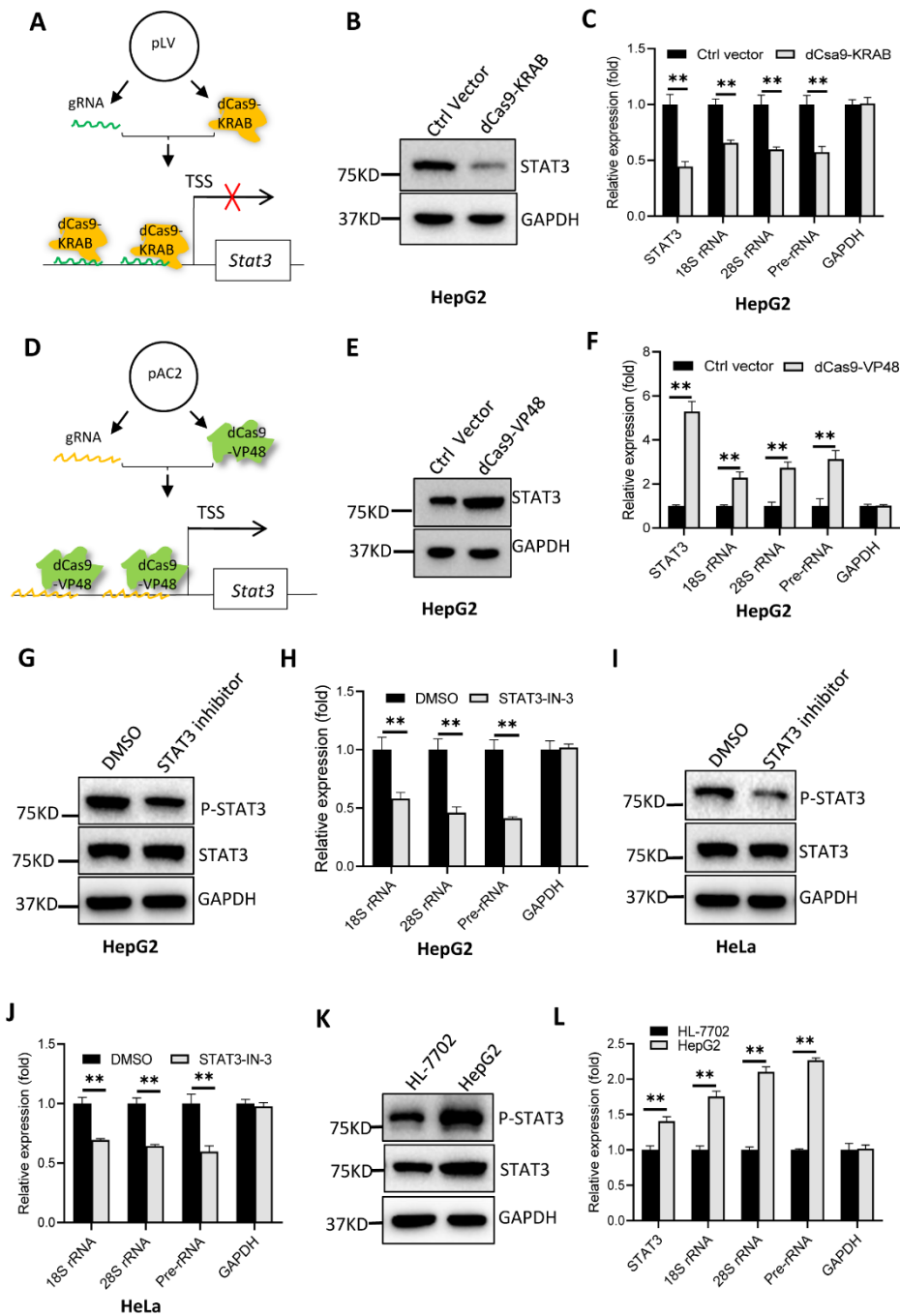
854

855 **Figure 1. Alteration of STAT3 expression affected Pol I-directed transcription. A**

856 **and B) STAT3 shRNA stable expression reduced Pol I-directed transcription in**

857 HepG2 cell lines. STAT3 expression was detected by Western blot (A), while Pol I
858 products were detected by RT-qPCR (B). C and D) mCherry-STAT3 stable expression
859 enhanced Pol I-directed transcription in HepG2 cells. mCherry-STAT3 (C) and Pol I
860 products (D) were analyzed by Western blot and RT-qPCR, respectively. E and F) EU
861 assay results for HepG2 cells with STAT3 silencing. EU assays were performed using
862 the cell lines as indicated, and images were captured under a confocal fluorescence
863 microscope (E). The scale bars in the images represent 5 μ m. Relative fluorescence
864 intensity for nucleoli in the images was calculated using ImageJ software (F). G and
865 H) EU assay results for HepG2 cells with STAT3 overexpression. EU assays were
866 performed using the cell lines as indicated. Images (G) and relative fluorescence
867 intensity for nucleoli (H) were obtained as described in E and F. I and J) Dot blot
868 results for the expression of pre-RNA in HepG2 cell lines expressing STAT3 shRNA
869 or control shRNA. J represents the quantified result for the dot blots obtained in I. K
870 and L) Dot blot results for the expression of pre-RNA in a HepG2 cell line expressing
871 mCherry-STAT3 (mCH-STAT3) or its control cell line. K represents the quantified
872 result for the dot blots obtained in L. Each column in histograms represents the
873 mean \pm SD of three independent experiments (n=3). *, $P<0.05$; **, $P<0.01$. P values
874 were obtained by Student's t test, performed with control and treatment groups.

Fig.2

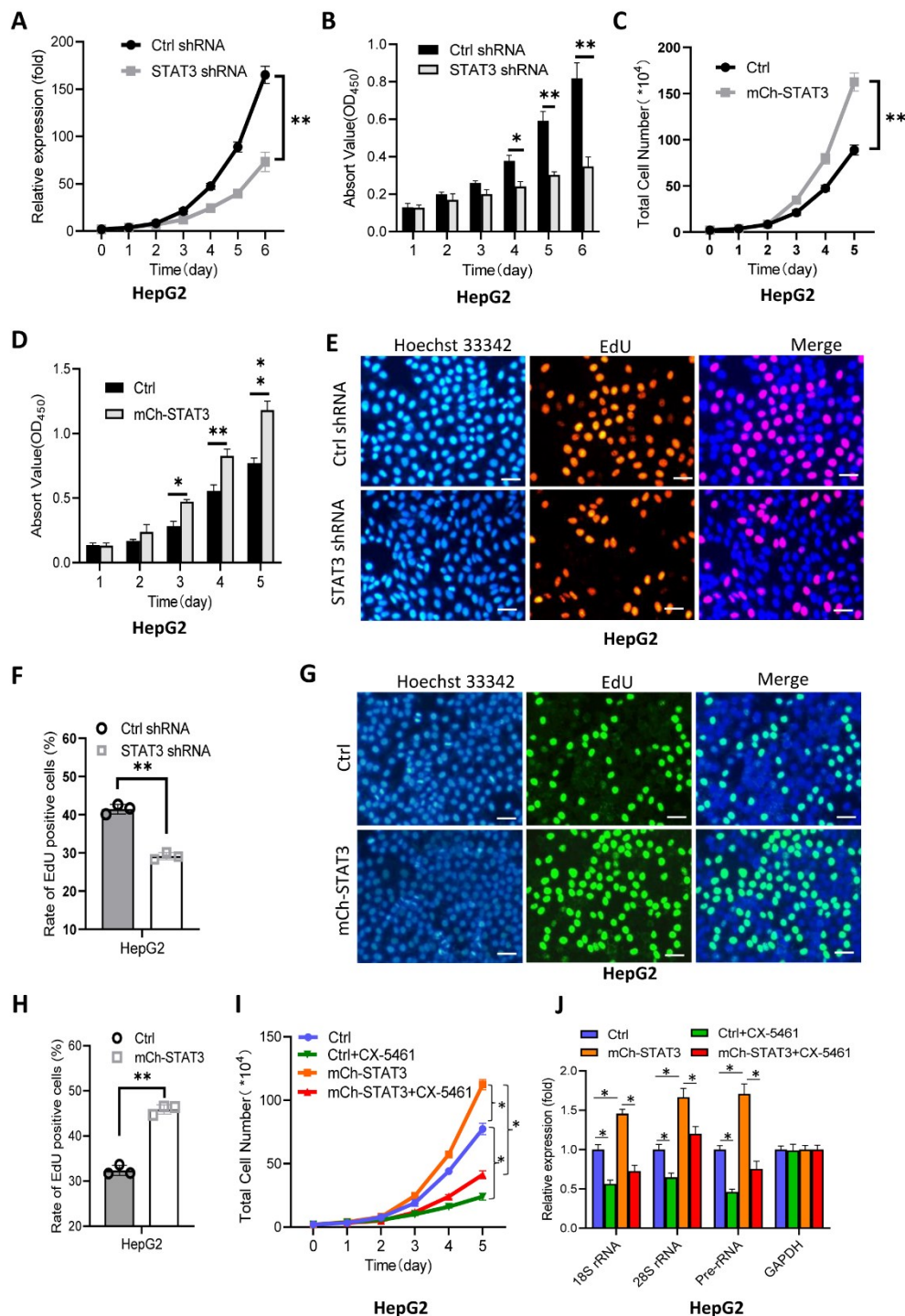


875

876 **Figure 2. The positive role of STAT3 in Pol I-directed transcription was**
 877 **confirmed by a dCas9 activation and repression system as well as a STAT3**
 878 **inhibitor. A)** A scheme showing the guide RNA (gRNA) and dCas9-KRAB that
 879 target the *STAT3* promoter region. **B)** STAT3 immunoblotting analysis in HepG2 cells
 880 transfected with the vectors expressing both STAT3 gRNAs and dCas9-KRAB or
 881 dCas9-KRAB only. **C)** Analysis of Pol I products by RT-qPCR using the cells
 882 obtained in B. **D)** A scheme showing guide RNA (gRNA) and dCas9-VP48 that target
 883 the *STAT3* promoter region. **E)** STAT3 expression analysis in HepG2 cells transfected
 884 with the vectors expressing both STAT3 gRNAs and dCas9-VP48 or dCas9-VP48

885 only by Western blot. **F)** Detection of Pol I products by RT-qPCR using the cells
886 obtained in E. **G)** Analysis of STAT3 expression and phosphorylation by Western blot
887 using HepG2 cells in the presence or absence of STAT3-IN-3 (2 μ M). **H)** The
888 presence of STAT3 inhibitor reduced Pol I product expression in HepG2 cells. **I)**
889 Analysis of STAT3 expression and phosphorylation by Western blot using HeLa cells
890 cultured in the medium with or without STAT3-IN-3 (2 μ M). **J)** The presence of
891 STAT3 inhibitor inhibited Pol I product expression in HeLa cells. **K)** Analysis of
892 STAT3 expression and phosphorylation by Western blot using HepG2 cells and its
893 primary (normal) cells (HL-7702). **L)** Comparison of Pol I product levels between
894 HL-7702 and HepG2 cells. Pol I products in H, J and L were detected by RT-qPCR.
895 Each column in histograms represents the mean \pm SD of three independent experiments
896 (n=3). *, $P<0.05$; **, $P<0.01$. P values were obtained by Student's t test,
897 performed with control and treatment groups.

Fig.3

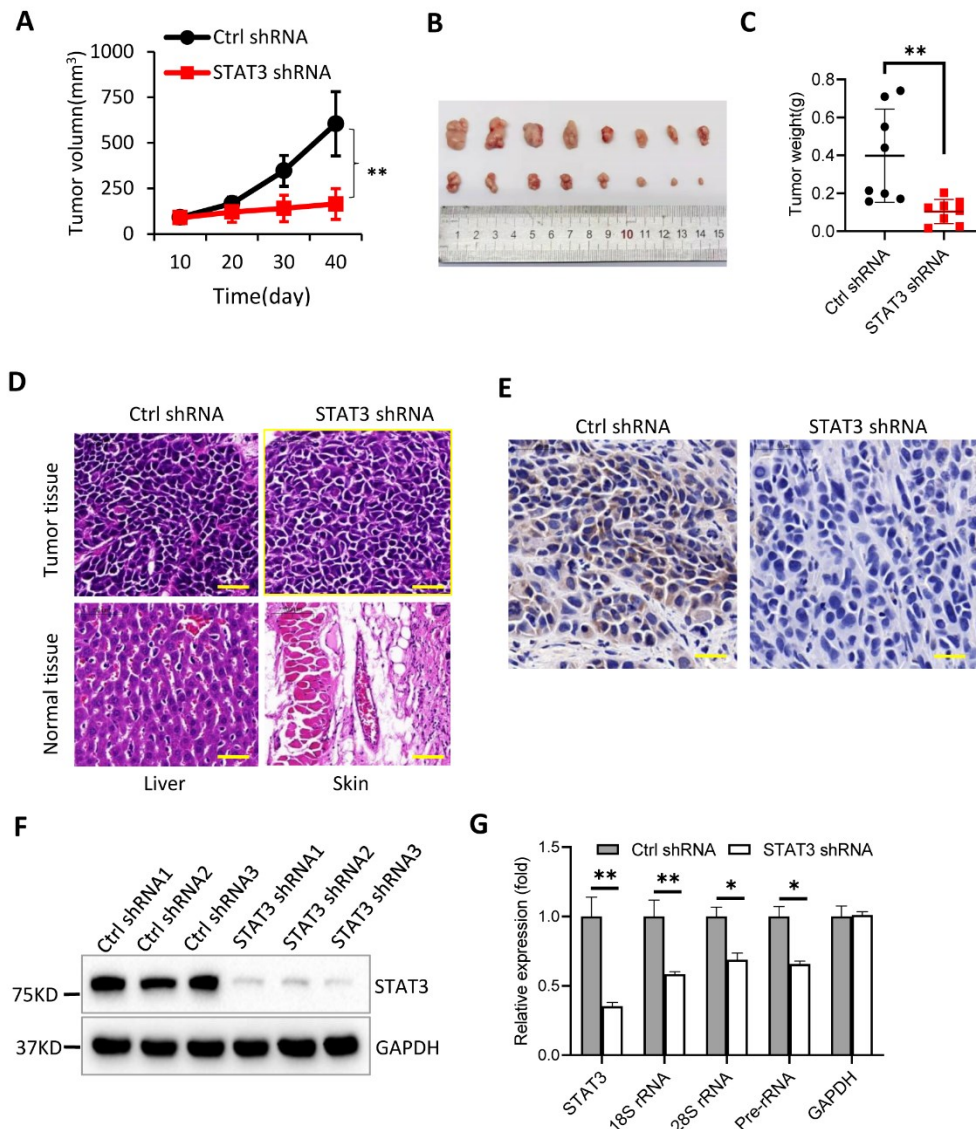


898

899 **Figure 3. STAT3 promotes cancer cell proliferation.** A and B) STAT3 knockdown
 900 reduced HepG2 cell proliferative activity. HepG2 cell lines expressing STAT3 shRNA
 901 or control shRNA were used to analyze proliferative activity by cell counting (A) and
 902 CCK-8 (B) methods. C and D) STAT3 overexpression enhanced HepG2 cell
 903 proliferative activity. Proliferation assays were performed by cell counting (C) and
 904 CCK-8 (D) methods using a HepG2 cell line stably expressing mCherry-STAT3 and

905 its control cell line. **E)** Representative images for EdU assays using HepG2 cell lines
906 stably expressing STAT3 shRNA or control shRNA. EdU specimens were observed
907 and imaged under a fluorescence microscope, the scale bars represent 50 μm . **F)**
908 Statistical analysis of the EdU-labeled cells based on the EdU assays described in (E).
909 The rate of EdU positive cells represents the number of EdU-labeled cells in the
910 number of total cells counted in the images. **G)** Representative images for EdU assays
911 using a HepG2 cell line expressing mCherry-STAT3 and its control cell line. Scale
912 bars in all images represents 50 μm . **H)** Statistical analysis of the EdU-labeled cells
913 based on the EdU assays described in G. The rate of the EdU positive cells was
914 obtained as for F. **I)** CX-5461 inhibited the enhancement of HepG2 cell proliferation
915 caused by STAT3 overexpression. Cell proliferation assays were performed using a
916 HepG2 cell line stably expressing mCherry-STAT3 and its control cell line, which
917 were cultured with or without CX-5461 (5 μM). **J)** CX-5461 inhibited the activation
918 of Pol I-directed transcription caused by STAT3 overexpression. HepG2 cell lines
919 treated with an inhibitor for 2 days were harvested for the analysis of Pol I products.
920 Each point/column in graphs represents the mean \pm SD of three independent
921 experiments (n=3). *, $P<0.05$; **, $P<0.01$. P values in A-D and I were obtained by
922 two-way ANOVA, P values in F, H and J were obtained by Student's t test, performed
923 with control and treatment groups.

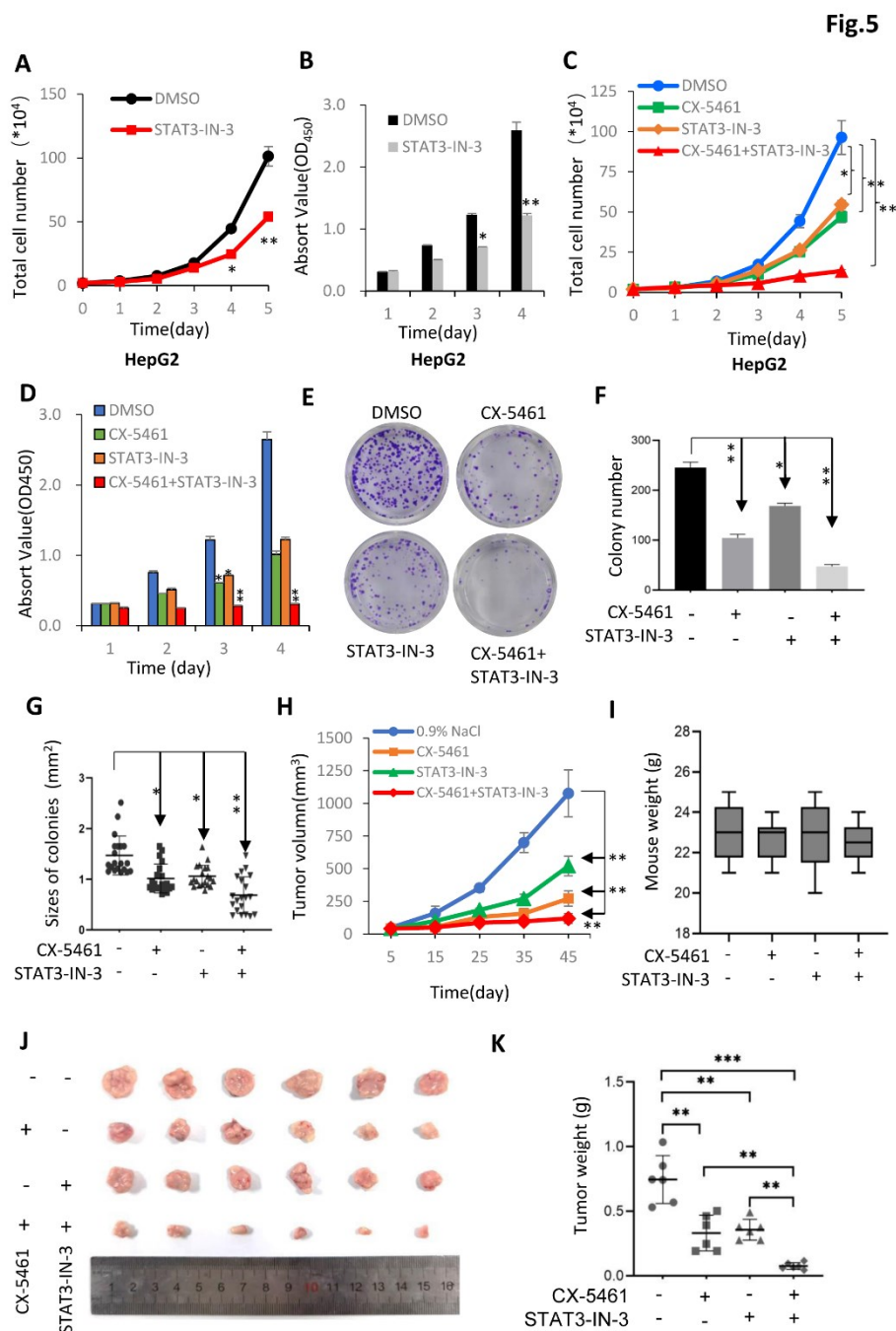
Fig.4



924

925 **Figure 4. STAT3 downregulation inhibited tumor cell growth *in vivo*.** A) STAT3
 926 knockdown reduced the sizes of tumors formed in nude mice. HepG2 cell lines
 927 expressing STAT3 shRNA or control RNA were subcutaneously injected into the back
 928 of nude mice (n=8). One week post-injection, tumors formed in mice were measured
 929 every 3 days until the mice were euthanized; the resulting data were subjected to
 930 statistical analysis. B) A image showing the effect of STAT3 downregulation on the
 931 tumor sizes formed in nude mice. C) STAT3 downregulation significantly reduced
 932 tumor weight. The tumors obtained in B were weighed and subjected to statistical
 933 analysis. D) Comparison of hematoxylin and eosin staining between tumor tissue and
 934 the normal tissues as indicated. The tissues from the tumor, liver or skin were fixed,
 935 sectioned and used for Hematoxylin and eosin staining. The scale bars in images
 936 represent 100 μ m. E) Immunohistochemistry images showing the difference of

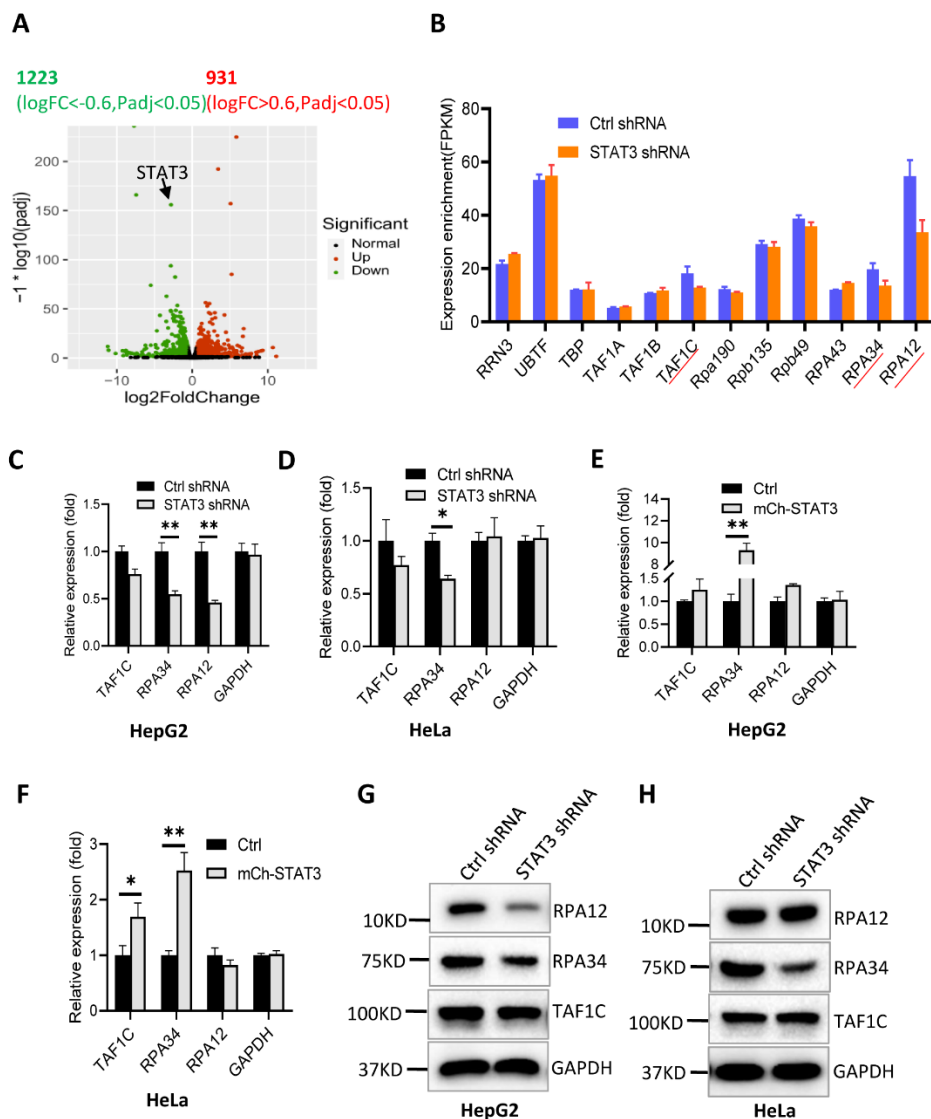
937 STAT3 expression between the tissues expressing STAT3 shRNA and control shRNA.
 938 **F)** Immunoblotting analysis of STAT3 expression in the tissues expressing STAT3
 939 shRNA or control shRNA. **G)** Analysis of Pol I products by RT-qPCR in the tissues
 940 expressing STAT3 shRNA or control shRNA. Each point/column in histograms
 941 represents the mean \pm SD of 8 biological replicates (n=8). *, $P < 0.05$; **, $P < 0.01$. P
 942 values obtained by two-way ANOVA (A) or Student's t test (C and G).



943
 944 **Figure 5. STAT3-IN-3 and CX-5461 showed an additive effect on the inhibition of**
 945 **tumor cell growth *in vitro* and *in vivo*.** **A and B)** The presence of STAT3-IN-3
 946 decreased HepG2 cell proliferation *in vitro*. Cell proliferation assays were performed
 947 using cell counting (A) and CCK-8 (B) methods. **C and D)** Effect of STAT3-IN-3 and

948 CX-5461 on tumor cell growth *in vitro*. HepG2 cell proliferation was measured with
 949 cell counting (C) and CCK-8 (D) methods. **E-G**) Effect of STAT3-IN-3 and CX-5461
 950 on the colony formation of HepG2 cells. Colony formation assays were performed
 951 using HepG2 cells treated with drugs as indicated. After 10 days, cells were subjected
 952 to fixation, staining and imaging (E); the number (F) and sizes (G) of colonies in the
 953 images were analysed statistically. **H**) A plot showing the volumes of tumors
 954 measured during tumor formation in the mice treated with different drugs. **I**) A graph
 955 showing the weights of the mice treated with different drugs after tumors were
 956 removed. **J**) An image showing the tumors obtained from the mice treated with
 957 different drugs. **K**) Statistical analysis of the tumors obtained from the mice treated
 958 with different drugs. Each point/column in histograms represents the mean±SD of
 959 three independent experiments (A-D) or 6 biological replicates (H, I and K). *,
 960 $P < 0.05$; **, $P < 0.01$. P values were obtained by two-way ANOVA (A-D and H) or
 961 Student's t test (F, G and K).

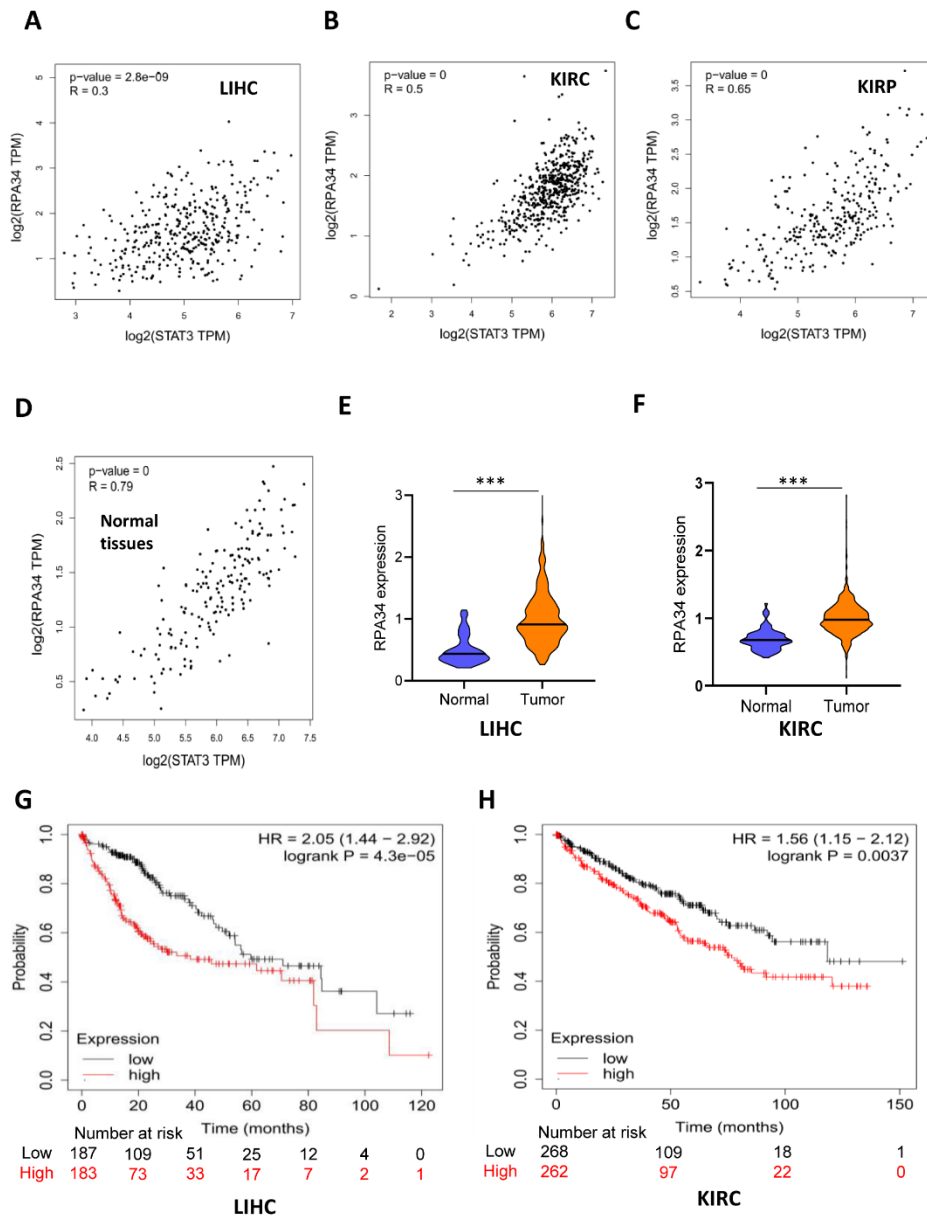
Fig 6



962

963 **Figure 6. STAT3 expression positively correlates with RPA34 expression at both**
964 **RNA and protein levels.** A) A volcano plot showing the number of upregulated and
965 downregulated differential expression genes (DEGs) based on the mRNA-seq data of
966 HepG2 cell lines expressing STAT3 shRNA or control shRNA. The significant DEGs
967 were defined by the differential expression that is over 1.5-fold between the reads of
968 STAT3 shRNA and control shRNA. B) Analysis of mRNA expression (FPKM) for the
969 genes encoding Pol I transcription machinery factors. The expression of genes
970 presented in the graph was analysed from the mRNA dataset detected by mRNA-seq,
971 where differential expression genes were underscored by red lines. C and D) RT-
972 qPCR was used to verify the effect of STAT3 silencing on mRNA expression of
973 RPA12, RPA34 and TAF1C in HepG2 (C) and HeLa (D) cells. E and F) RT-qPCR
974 was used to analyze the effect of STAT3 overexpression on the expression of RPA12,
975 RPA34 and TAF1C in HepG2 (E) and HeLa (F) cells. G and H) Western blot results
976 showing the effect of STAT3 knockdown on the expression of RPA12, RPA34 and
977 TAF1C in HepG2 (G) and HeLa (H) cells. Each point/column in digital graphs
978 represents the mean±SD of three biological replicates (A, B) or three independent
979 experiments (C-F). *, $P<0.05$; **, $P<0.01$. P values were obtained by Student's t test,
980 performed with control and treatment groups.

Fig. 7

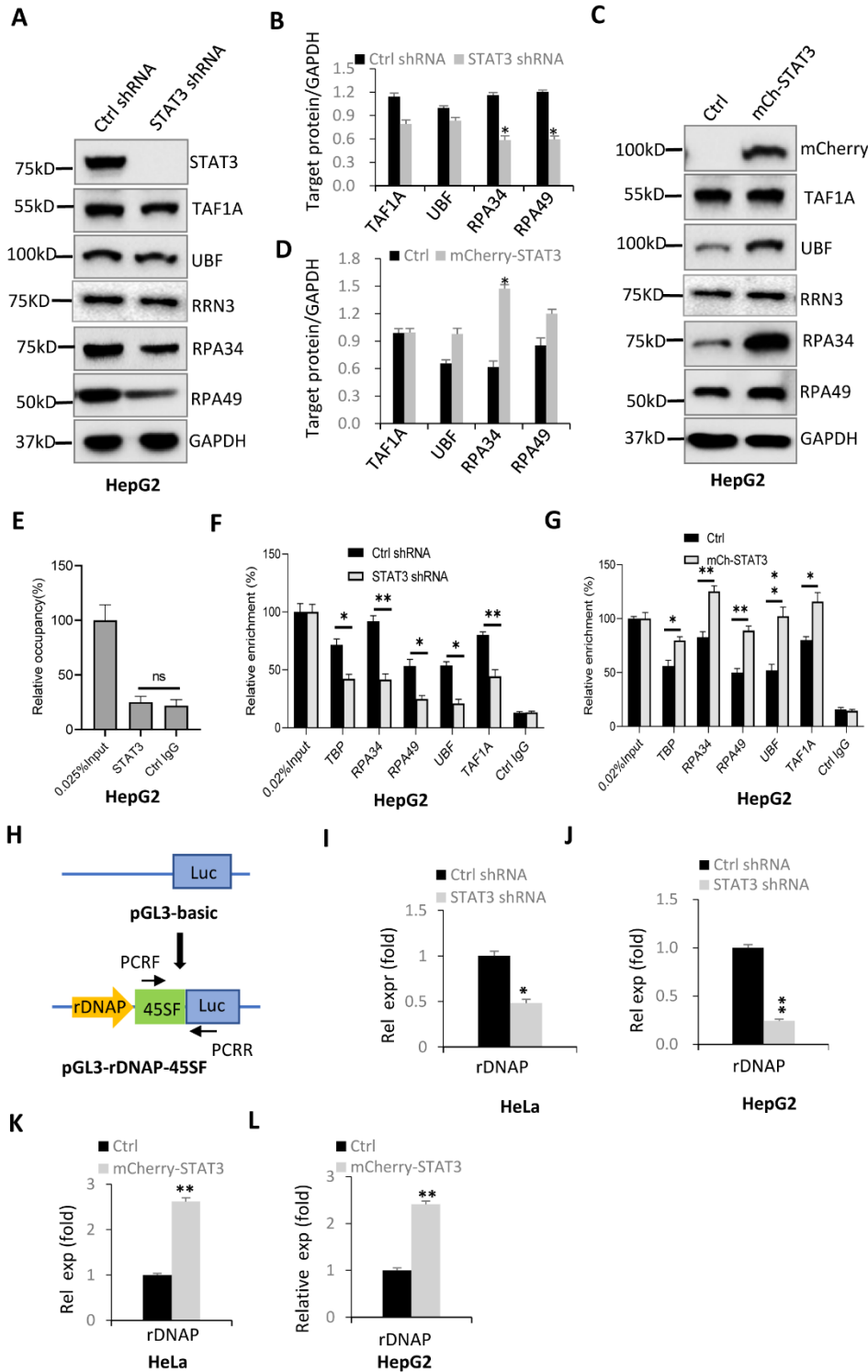


981

982 **Figure 7. The relationship between RPA34 expression levels and survival**
 983 **probability and survival time in cancers.** A-C) Pearson correlation analysis based
 984 on the TCGA dataset of clinical cancer samples, including liver hepatocellular
 985 carcinoma (LIHC), kidney renal clear cell carcinoma (KIRC) and kidney renal
 986 papillary cell carcinoma (KIRP), using the GEPIA online tool ([http://gepia2.cancer-](http://gepia2.cancer-pku.cn/#index)
 987 [pku.cn/#index](http://gepia2.cancer-pku.cn/#index)). D) Pearson correlation analysis based on the TCGA dataset of normal
 988 tissues, including liver, cervix and kidney tissues using the GEPIA online tool
 989 (<http://gepia2.cancer-pku.cn/#index>). E and F) Violin plots showing RPA34
 990 expression differentiation between normal tissues and liver hepatocellular carcinomas
 991 (LIHC) or Kidney renal carcinomas (KIRC). G and H) Kaplan-Meier Plots showing
 992 the relationship between RPA34 expression levels and survival probability and

993 survival time based on the TCGA dataset of liver hepatocellular carcinomas (LIHC)
 994 and Kidney renal carcinoma (KIRC). Low: RPA34 low expression, High: RPA34 high
 995 expression. High and Low expression levels were determined by the expression
 996 median of cancer samples. ***, $P < 0.001$, P values were obtained by Student's t test
 997 performed by normal and cancer samples (E, F).

Fig.8



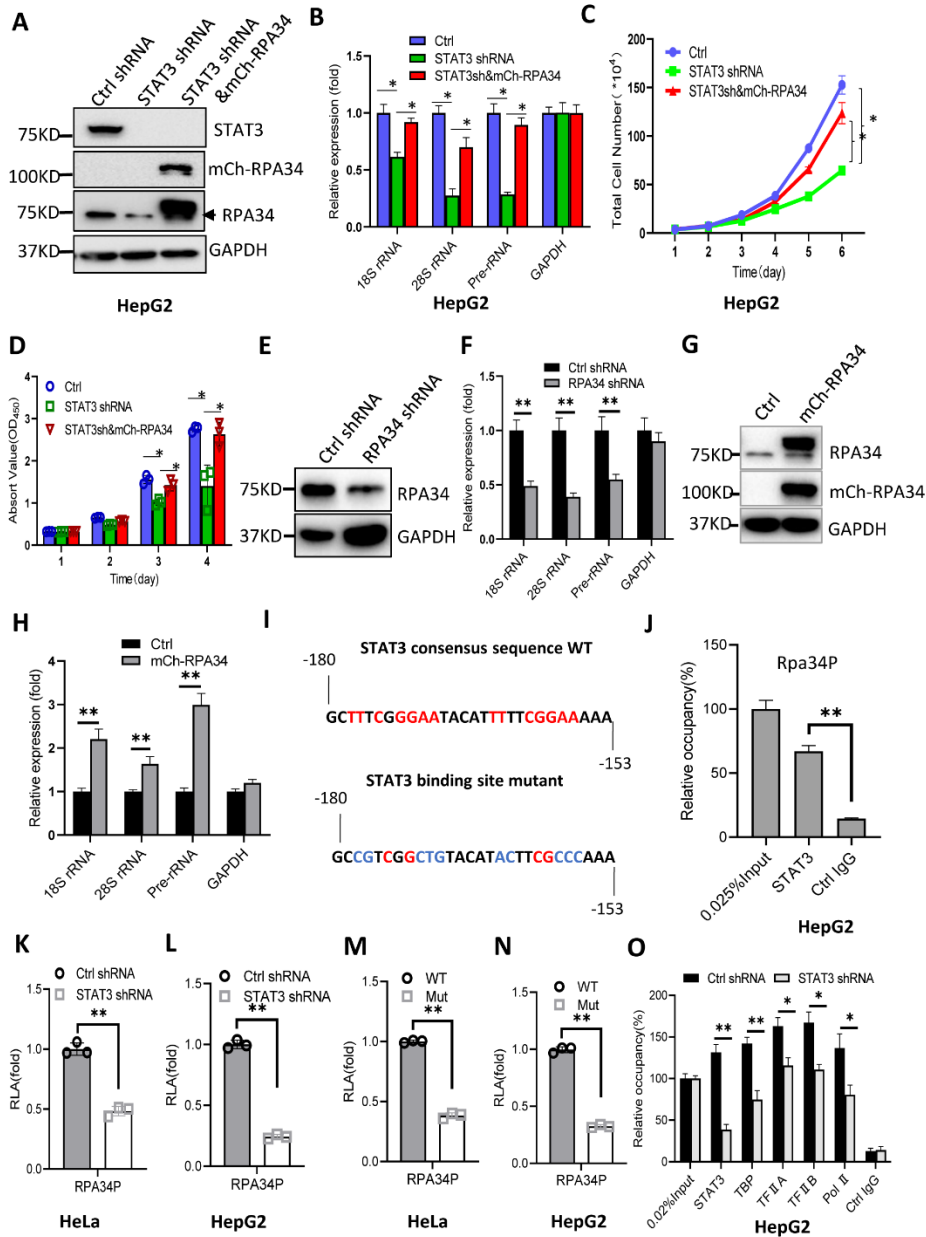
998

999

Figure 8. STAT3 regulates the assembly of components of the Pol I transcription

1000 **machinery at the rDNA promoter by affecting RPA34 expression. A and B)** Effect
1001 of STAT3 knockdown on the expression of the Pol I-related factors was analyzed by
1002 Western blot using HepG2 cells expressing STAT3 shRNA or control shRNA and
1003 antibodies as indicated (A). The quantified result of Western blots (n=3) is shown in
1004 B. **C and D)** Effect of STAT3 overexpression on the expression of Pol I-related factors
1005 by Western blot using HepG2 cells with STAT3 overexpression. D represents the
1006 quantified result of Western blots in C (n=3). **E)** STAT3 does not bind to the rDNA
1007 promoter. HepG2 cells were used for ChIP assays using an anti-STAT3 antibody,
1008 where the DNA recovered from the chromatin immunoprecipitation was analyzed by
1009 qPCR. Relative enrichment was obtained by comparing the relative quantity of target
1010 DNA in 1 μ L of ChIP samples to that from 0.025% input. **F)** STAT3 downregulation
1011 reduced the occupancies of the Pol I transcription machinery factors at the rDNA
1012 promoter. ChIP assays were performed using HepG2 cell lines expressing STAT3
1013 shRNA or control shRNA and antibodies against the factors as indicated. **G)** STAT3
1014 upregulation increased the occupancies of the Pol I transcription machinery factors at
1015 the rDNA promoter. ChIP assays were performed using a HepG2 cell line expressing
1016 mCherry-STAT3 and its control cell line in which antibodies against factors used for
1017 the assays were as indicated. **H)** A scheme showing the cloning of the rDNA promoter
1018 (rDNAP) with the reporter vector pGL3-basic. 45SF: 45S DNA fragment; Luc:
1019 luciferase. **I and J)** STAT3 knockdown inhibited the rDNA promoter activity. The
1020 ‘Reporter’ gene expression was detected by RT-qPCR using the primers as indicated
1021 in H after transfection of the rDNA promoter (rDNAP)-driving reporter vectors into
1022 HeLa (I) or HepG2 (J) cell lines. Rel exp: relative expression. **K and L)** STAT3
1023 overexpression inhibited the rDNA promoter activity. The ‘Reporter’ gene expression
1024 was monitored by RT-qPCR after transfecting the rDNA promoter-driving reporter
1025 vectors into HeLa (K) and HepG2 (L) cell lines. Each column in histograms
1026 represents the mean \pm SD of three independent experiments. *, $P < 0.05$; **, $P < 0.01$. P
1027 values were obtained by Student’s t test.

Fig.9



1028

1029 **Figure 9. STAT3 modulates Pol I-directed transcription by controlling RPA34**

1030 **transcription. A)** Generation of HepG2 cell lines stably expressing both STAT3

1031 shRNA and mCherry-RPA34. Western blot was used to verify HepG2 cell lines

1032 expressing STAT3 shRNA only or both STAT3 and mCherry-STAT3 and the control

1033 cell line using antibodies as indicated. **B)** Analysis of Pol I products by RT-qPCR

1034 using the cell lines established in A. **C** and **D)** Cell proliferation assays for the cell

1035 lines established in (A). Cell proliferation assays were performed using cell counting

1036 (C) and CCK-8 (D) methods. **E** and **F)** Effect of RPA34 silencing on Pol I-directed

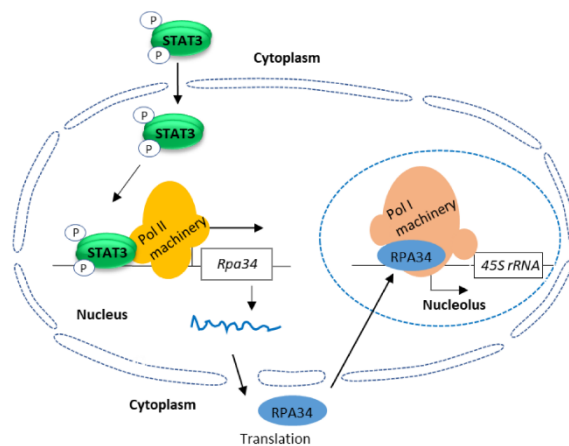
1037 transcription in HepG2 cells. RPA34 and Pol I products were analyzed by Western

1038 blot (E) and RT-qPCR (F), respectively. **G** and **H)** Effect of RPA34 overexpression on

1039 Pol I-directed transcription in HepG2 cells. RPA34 and Pol I products were analyzed

1040 by Western blot (G) and RT-qPCR (H), respectively. **I)** A cartoon showing putative
 1041 STAT3 binding elements in the *Rpa34* promoter. Red letters represent STAT3
 1042 consensus bases (WT), while blue letters represent the mutations of STAT3 consensus
 1043 bases. **J)** A ChIP result showing the STAT3 occupancy at the *Rpa34* promoter in
 1044 HepG2 cells. **K and L)** STAT3 inhibited the *Rpa34* promoter activity in HeLa and
 1045 HepG2 cells. Luciferase assays were performed by transfecting the RPA34P-driving
 1046 reporter vectors into HeLa and HepG2 cell lines expressing STAT3 shRNA or control
 1047 shRNA. Relative luciferase activity (RLA) was obtained by comparing the luciferase
 1048 activity of treatment samples to that of control samples, where the activity of control
 1049 samples was arbitrarily set as 1. **M and N)** Mutations of the STAT3 consensus bases
 1050 suppressed the *Rpa34* promoter activity. The reporter vectors driven by the wild type
 1051 RPA34P or by its mutant containing STAT3-binding site mutations were transfected
 1052 into HeLa and HepG2 cells. RLA, relative luciferase activity. **O)** STAT3
 1053 downregulation inhibited the occupancies of the Pol II transcription machinery factors
 1054 at the *Rpa34* promoter. ChIP assays were performed using HepG2 cell lines
 1055 expressing STAT3 shRNA or control shRNA and the antibodies against the factors as
 1056 indicated. The relative occupancy was obtained as described in Fig. 6A. Each column
 1057 in the histograms represents the mean \pm SD of three independent experiments. *,
 1058 $P < 0.05$; **, $P < 0.01$. P values were obtained by two-way ANOVA (B-D) or Student's t
 1059 test (F,H,J-O).

Fig.10



1060
 1061 **Figure 10. A proposed model by which STAT3 modulates Pol I-directed**
 1062 **transcription.** After phosphorylation, p-STAT3 enters nuclei and binds to the *Rpa34*
 1063 promoter to transcribe RPA34 mRNA. After translation, RPA34 protein enters
 1064 nucleoli and binds to the rDNA promoter to initiate Pol I-directed transcription.